# Regge Poles in Resonance Production*

ROBERT L. THEWS†
*Laboratory for Nuclear Science and Physics Department, Massachusetts Institute of Technology, Cambridge, Massachusetts*

(Received 19 August 1966; revised manuscript received 31 October 1966)

The theory of Regge trajectory exchange is applied to the high-energy production of meson and baryon resonances. The helicity representation is used for the production amplitudes. The predictions are compared with experimental data on production of the $N^*(1238)$ nucleon resonance by pions and kaons, and also the production of the $f^0$ and $\rho$ mesons by pions. The energy dependence of the differential cross sections is found to be consistent with the Regge-pole exchange model. Values for the $\rho$, $A_2$, and $\pi$ trajectories are determined. The $\rho$ and $A_2$ values are compared with those determined by analysis of elastic and charge-exchange scattering data. The $\pi$ trajectory values have not been determined in other reactions, but they are consistent with the known general properties of Regge trajectories. The spin density matrix elements are not strongly restricted by the theory, but the predictions that can be made are also consistent with experiment.

## I. INTRODUCTION AND SUMMARY OF RESULTS

THE predictions of the Regge-pole exchange model have been compared with data on elastic scattering of strongly interacting particles at high energies.[1,2] The success of these predictions does not provide a very stringent test of the theory, however, since at least five poles are needed, and there are a large number of free parameters to be determined. A better test is provided by meson-nucleon charge-exchange scattering,[1,3–5] in which conservation laws severely limit the number of poles which can be exchanged. Successful predictions are also made for $\eta$ production by pions,[6] meson-nucleon and nucleon-nucleon total cross sections,[7] and pion-nucleon backward scattering.[8] Another class of reactions in which the number of exchanged poles is restricted is the production of meson and baryon resonances in quasi-two-body events.

A large quantity of data is becoming available on resonance production cross sections at laboratory energies from 2 to 10 GeV. There are two features which characterize almost all of these reactions. The first is a diffraction peak in the differential cross section, favoring small momentum transfer between the incoming meson and meson resonance, and the target baryon and baryon resonance. The second general feature is the energy variation of the production cross section, which rises from zero at threshold to a maximum at about 1–3 GeV, and then decreases with energy above this point. The object of this paper is to compare these data with the predictions of the Regge-pole exchange model, and to determine the Regge trajectory parameters where possible. A comparison of these parameters with those determined from elastic and charge-exchange scattering provides a further test of the Regge-pole model.

Section II is devoted to the Regge-pole formalism for particles with arbitrary spin. Using the helicity representation, the high-energy behavior of production amplitudes is deduced, and the dominance of the Regge-pole terms is established. In Sec. III, data on the reactions $\pi^+ + p \to \pi^0 + N^*$, $K^+ + p \to K^0 + N^*$, $\pi^- + p \to f^0 + n$, and $\pi^+ + p \to \rho^+ + p$ are compared with the predictions of Regge-pole exchange. Values for the $\rho$, $A_2$, and $\pi$ Regge trajectories are determined. Some useful kinematical relationships, along with properties of helicity amplitudes and Regge-pole terms, are presented in an appendix.

The main conclusion of this analysis is that the energy dependence of the differential cross sections for meson and baryon resonances in a quasi-two-body reaction is consistent with the exchange of a small number of Regge trajectories. The trajectory parameters can be determined from the experimental data, and the values obtained are consistent with those found by analysis of elastic and charge-exchange scattering. The requirements imposed on the spin density matrix elements are not as stringent as those imposed by single-particle exchange, but their energy variation (or lack of it) is well reproduced, and their values are consistent with those restrictions. The main assumptions and results are summarized below.

### Assumptions

(1) The helicity amplitudes for resonance production can be written as single dispersion relations in either energy or momentum transfer.

(2) The partial-wave amplitudes have simple poles which move with energy in the complex angular momentum plane.

(3) There are no fixed poles in angular momentum.

(4) If cuts in angular momentum occur, their con-

* This work is supported in part through funds provided by the U. S. Atomic Energy Commission under Contract No. AT(30-1)-2098.

† Present address: University of California, Lawrence Radiation Laboratory, Berkeley, California.

[1] R. J. N. Phillips and W. Rarita, Phys. Rev. **139**, B1336 (1965).
[2] K. J. Foley, S. J. Lindenbaum, W. A. Love, S. Ozaki, J. J. Russell, and C. L. Yuan, Phys. Rev. Letters **10**, 376 (1963).
[3] R. K. Logan, Phys. Rev. Letters **14**, 414 (1965).
[4] G. Höhler, J. Baacke, H. Schaile, and P. Sonderegger, Phys. Letters **20**, 79 (1966).
[5] F. Arbab and C. Chiu, Phys. Rev. **147**, 1045 (1966).
[6] R. J. N. Phillips and W. Rarita, Phys. Rev. **140**, B200 (1965).
[7] V. Barger and M. Olsson, Phys. Rev. **146**, 1080 (1966).
[8] V. Barger and D. Cline, Phys. Rev. Letters **16**, 913 (1966).

tribution to high-energy cross sections is either negligible or indistinguishable from that of a single pole at some position.

(5) The partial-wave amplitudes satisfy a certain symmetry relation (the Mandelstam symmetry) which allows the pole terms to dominate the high-energy amplitudes for all trajectory values.

### Results

(1) The production of $N^*(1238)$ by pions can be explained by $\rho$ Regge trajectory exchange. The trajectory values obtained are consistent with those found by analysis of elastic and charge-exchange $\pi p$ scattering. Since the helicity amplitudes all have the same phase, a relationship is predicted for the spin density matrix elements, and this is in agreement with experiment. The energy variation of the matrix elements is small, also in agreement with the Regge trajectory exchange theory.

(2) The production of $N^*$ by kaons can be explained by a combination of $\rho$ and $R$ trajectory exchange, with the $R$ exchange contributing the major part. To separate the $\rho$ contribution, exact $SU(3)$ symmetry was assumed for the $\rho\pi\pi$ and $\rho KK$ couplings. The trajectory values determined for the $R$ agree with those from elastic and charge-exchange scattering results, except in the small momentum transfer region, where the kinematical approximations are less accurate. The spin density matrix element predictions are the same as above, in the approximation of $R$ trajectory dominance, and are consistent with experimental values.

(3) The production of the $f^0$ by pions can be explained by the exchange of a $\pi$ Regge trajectory alone. The trajectory values obtained are negative and can easily be extrapolated to go through the square of the pion mass at zero angular momentum. There are no other values with which to compare these, since the small trajectory value indicates that pion exchange may be neglected in elastic scattering. An extrapolation of the pion residue function reveals that a rapid variation is necessary for agreement of the Regge exchange amplitude with the field-theoretic amplitude at the physical pion pole. The spin density matrix elements are in agreement with the limited data available.

(4) The production of $\rho$ mesons by pions can be explained by a combination of $\pi$ and $\omega$ trajectory exchange with the $\pi$ contribution dominant at low energies, but the $\omega$ contribution growing in importance as the energy increases. The model is also supported by the results for $\rho^0$ production, due to $\pi$ exchange alone. The extrapolation of the pion residue function to the physical pion pole again requires rapid variation. The values and energy variation of the spin density matrix elements are in agreement with experiment.

## II. REGGE-POLE FORMALISM

The starting point for the examination of the high-energy behavior of the $s$-channel reaction $A+B\to C+D$ is the partial-wave expansion of the amplitudes for the $t$-channel reaction $A+\bar{C}\to\bar{B}+D$. In the helicity representation of Jacob and Wick,[9] this is

$$M_{\lambda_A\lambda_{\bar{C}},\lambda_{\bar{B}}\lambda_D}(t,x)=(-1)^{\lambda'-\lambda}\sum_{J=\lambda}^{\infty}(J+\tfrac{1}{2})A^J{}_{\lambda_A\lambda_{\bar{C}},\lambda_{\bar{B}}\lambda_D}(t)d^J{}_{\lambda\lambda'}(x), \quad (1)$$

where the $\lambda$'s are the particle helicities, $\lambda=\lambda_A-\lambda_{\bar{C}}$, $\lambda'=\lambda_{\bar{B}}-\lambda_D$, $t$ is the square of the center-of-mass energy, $x$ is the cosine of the angle between particles $A$ and $\bar{C}$, $A^J{}_{\lambda_A\lambda_{\bar{C}},\lambda_{\bar{B}}\lambda_D}(t)$ is the partial-wave amplitude, and $d^J{}_{\lambda\lambda'}(x)$ is the rotation coefficient for total angular momentum $J$. The factor $(-1)^{\lambda-\lambda'}$ is taken out so that the $d^J{}_{\lambda\lambda'}$ functions agree with the phase convention of Andrews and Gunson.[10] It is assumed in the following that $\lambda\geq|\lambda'|$, but the results can easily be extended to other values by using symmetry properties of the rotation coefficients.[5] The next step is the continuation of the $A^J$ and $d^J$ functions to complex values of $J$, and the use of the Sommerfeld-Watson transformation to convert the $J$ sum into an integral in the complex $J$ plane. This development is essentially the same as that of Calogero, Charap, and Squires.[11]

The $d^J{}_{\lambda\lambda'}$ functions can be continued through their connection with the hypergeometric function (see Appendix). The continuation of the partial-wave amplitudes is defined in analogy with the Froissart-Gribov continuation.[12,13] The orthogonality of the $d^J{}_{\lambda\lambda'}$ is used to invert (1). For simplicity, we abbreviate $\lambda_A\lambda_{\bar{C}}$ by $\lambda$ and $\lambda_{\bar{B}}\lambda_D$ by $\lambda'$.

$$A^J{}_{\lambda\lambda'}(t)=\int_{-1}^{1}M_{\lambda\lambda'}(t,x)d^J{}_{\lambda\lambda'}(x)dx. \quad (2)$$

We now put in analyticity through the assumption

$$M_{\lambda\lambda'}(t,x)=\left(\frac{1+x}{2}\right)^{(\lambda+\lambda')/2}\left(\frac{1-x}{2}\right)^{(\lambda-\lambda')/2}\left\{\frac{1}{\pi}\int_{z_0^s}^{\infty}\frac{A^s{}_{\lambda\lambda'}(t,s(z))}{z-x}dz+\frac{1}{\pi}\int_{z_0^u}^{\infty}\frac{A^u{}_{\lambda\lambda'}(t,u(-z))}{z+x}dz\right\}. \quad (3)$$

[9] M. Jacob and G. C. Wick, Ann. Phys. (N. Y.) 7, 404 (1959).
[10] M. Andrews and J. Gunson, J. Math. Phys. 5, 1391 (1964).
[11] F. Calogero, J. M. Charap, and E. J. Squires, Ann. Phys. (N.Y.) 25, 325 (1963).
[12] M. Froissart, La Jolla Conference on Strong and Weak Interactions, 1961 (unpublished).
[13] V. N. Gribov, Zh. Eksperim. i Teor. Fiz. 41, 667 (1961); 41, 1962 (1961) [English transls.: Soviet Phys.—JETP 14, 478 (1962); 14, 1395 (1962)].

When (3) is inserted into (2), the integral over $x$ can be done immediately, and yields

$$A^J{}_{\lambda\lambda'}(t)=\frac{2}{\pi}\int_{z_0{}^s}^{\infty}A^s{}_{\lambda\lambda'}(t,s(z))\left(\frac{1+z}{2}\right)^{(\lambda+\lambda')/2}\left(\frac{1-z}{2}\right)^{(\lambda-\lambda')/2}e^J{}_{\lambda\lambda'}(z)dz$$
$$+(-1)^{J-\lambda}\frac{2}{\pi}\int_{z_0{}^u}^{\infty}A^u{}_{\lambda\lambda'}(t,u(-z))\left(\frac{1+z}{2}\right)^{(\lambda-\lambda')/2}\left(\frac{1-z}{2}\right)^{(\lambda+\lambda')/2}e^J{}_{\lambda,-\lambda'}(z)dz, \quad (4)$$

where the $e^J{}_{\lambda\lambda'}$ are rotation coefficients of the second kind, and we have used

$$e^J{}_{\lambda\lambda'}(-z)=-(-1)^{J-\lambda}e^J{}_{\lambda,-\lambda'}(z) \quad (5a)$$

for $J-\lambda$ integer. If the dispersion integrals are to converge with a finite number of subtractions, $M_{\lambda\lambda'}(t,x)$ must be bounded by a power of $x$ as $|x|\to\infty$,

$$|M_{\lambda\lambda'}(t,x)x^{-\alpha}|\xrightarrow[|x|\to\infty]{}0. \quad (5b)$$

This implies that the weight functions in (3) must be bounded by $x^{\alpha-\lambda}$, and since $e^J{}_{\lambda\lambda'}(x)$ is bounded by $x^{-J-1}$, we see that the integrals in (4) converge for $J>\alpha$. Subtraction terms in the dispersion relation (3) do not contribute to $A^J{}_{\lambda\lambda'}(t)$ for $J>\alpha$. Of interest for the Sommerfeld-Watson transformation is the large $J$ behavior of the partial-wave amplitudes. Asymptotically, $e^J{}_{\lambda\lambda'}(x)\sim e^{-\epsilon J}/J^{1/2}$ as $|J|\to\infty$, where $\epsilon>0$ for $x>1$. In terms of $s$ and $t$, $x$ can be written as

$$x=\frac{2t(s-M_A{}^2-M_B{}^2)+(t+M_A{}^2-M_C{}^2)(t+M_B{}^2-M_D{}^2)}{[(t-M_A{}^2-M_C{}^2)^2-4M_A{}^2M_C{}^2]^{1/2}[(t-M_B{}^2-M_D{}^2)^2-4M_B{}^2M_D{}^2]^{1/2}}. \quad (6)$$

For $t\geq t_0$ ($t$-channel threshold), it can be shown that $x>1$ for $s>0$, $x<-1$ for $u<0$, provided that $(M_A{}^2-M_C{}^2)\times(M_B{}^2-M_D{}^2)\geq 0$. This last condition, by our convention (1), is true for elastic scattering and resonance production, so that the partial-wave amplitudes $A^J{}_{\lambda\lambda'}(t)$ are bounded by a decreasing exponential for large $|J|$. The factor $(-1)^{J-\lambda}$ is not convergent as $\mathrm{Im}J\to\infty$, so that two separate continuations must be defined, and the concept of signature is introduced. If we define $A^{\pm}{}_{\lambda\lambda'}(t,J)$ by Eq. (4) with the factor $(-1)^{J-\lambda}$ replaced by $\pm$, then

$$A^+{}_{\lambda\lambda'}(t,J)=A^J{}_{\lambda\lambda'}(t) \quad \text{for } J-\lambda \text{ even integer}, \quad (7a)$$

and

$$A^-{}_{\lambda\lambda'}(t,J)=A^J{}_{\lambda\lambda'}(t) \quad \text{for } J-\lambda \text{ odd integer}. \quad (7b)$$

It is then convenient to define two functions $d^{\pm}{}_{\lambda\lambda'}(x,J)$ by the relation

$$d^{\pm}{}_{\lambda\lambda'}(x,J)=\tfrac{1}{2}[d^J{}_{\lambda\lambda'}(x)\pm d^J{}_{\lambda,-\lambda'}(-x)]. \quad (8)$$

The partial-wave expansion (1) can then be written

$$M_{\lambda\lambda'}(t,x)=(-1)^{\lambda-\lambda'}\sum_{J=\lambda}^{\infty}(J+\tfrac{1}{2})[A^+{}_{\lambda\lambda'}(t,J)d^+{}_{\lambda\lambda'}(x,J)+A^-{}_{\lambda\lambda'}(t,J)d^-{}_{\lambda\lambda'}(x,J)]. \quad (9)$$

The $A^{\pm}$ and $d^{\pm}$ functions are in a form suitable for the Sommerfeld-Watson transformation:

$$M_{\lambda\lambda'}(t,x)=(-1)^{\lambda-\lambda'}\sum_{J=\lambda}^{N}(J+\tfrac{1}{2})A^J{}_{\lambda\lambda'}(t)d^J{}_{\lambda\lambda'}(x)$$
$$-\frac{(-1)^{\lambda-\lambda'}}{2\pi i}\int_C\frac{dJ(J+\frac{1}{2})\pi}{\sin\pi(J-\lambda)}[A^+{}_{\lambda\lambda'}(t,J)d^+{}_{\lambda,-\lambda'}(-x,J)+A^-{}_{\lambda\lambda'}(t,J)d^-{}_{\lambda,-\lambda'}(-x,J)], \quad (10)$$

where $N-1<\alpha<N$, with $\alpha$ defined by (5b), and the contour $C$ consists of the line $\mathrm{Re}J=N+\frac{1}{2}$ and an infinite semicircle in the right-half $J$ plane. The $A^{\pm}{}_{\lambda\lambda'}(t,J)$ have no singularities in $J$ for $J>\alpha$, and the $d^{\pm}{}_{\lambda\lambda'}(-x,J)$ have no singularities in $J$ except for branch points in the region $-\lambda\leq J\leq\lambda-1$, which is outside the contour. For large $|J|$, $d^J{}_{\lambda\lambda'}(x)\sim e^{\theta|\mathrm{Im}J|}/J^{1/2}$, where $\cos\theta=x$. Since $A^{\pm}{}_{\lambda\lambda'}(t,J)$ is bounded by $e^{-\epsilon J}/J^{1/2}$, we see that the integral is bounded by a decreasing exponential as $|J|\to\infty$, in the region $0\leq\theta\leq\pi$ and $t\geq t_0$, the physical $t$-channel region. Thus the semicircular part of the contour integral vanishes, and the only contribution is along $\mathrm{Re}J=N+\frac{1}{2}$. Next, the contour is pushed to the left in the $J$ plane to $\mathrm{Re}J=-\frac{1}{2}$. We assume that in the region $\mathrm{Re}J<\alpha$, the partial-wave amplitudes $A^{\pm}{}_{\lambda\lambda'}(t,J)$ have only simple poles in $J$ which move with energy, the Regge poles. The position of a pole is denoted by $\alpha(t)$, and the residue by $\beta^{\pm}{}_{\lambda\lambda'}(t)$. The factor $1/\sin\pi(J-\lambda)$ has poles at integer $J-\lambda$. The terms

from $J=\lambda$ to $J=N$ cancel the first part of the original partial-wave sum. The remaining terms from $J=0$ to $J=\lambda-1$ give terms proportional to $d^J{}_{\lambda\lambda'}(x)$. However, for integer $J-\lambda$ in the range $\lambda'\leq J\leq\lambda-1$, $d^J{}_{\lambda\lambda'}\equiv 0$, so that only the terms from $J=0$ to $J=\lambda'-1$ remain. The branch points in the $d^J{}_{\lambda\lambda'}$ functions are now included in the contour of integration. However, these occur only in the normalization factors (see Appendix), and the same factors appear in the partial-wave amplitudes due to the $e^J$ function. These branch points cancel, and the only singularities left are fixed poles in $J$ for integer $J-\lambda$, at positions $J=-n\pm\lambda'-1$, where $n$ is zero or a positive integer. Since, by assumption, fixed poles are not permitted, restrictions must be placed on the continuation of the partial-wave amplitudes. These are of the form

$$\int_{z_0}^{\infty} A^{s,u}{}_{\lambda\lambda'}(t,\cdots)\left(\frac{1+z}{2}\right)^{(\lambda\pm\lambda')/2}\left(\frac{1-z}{2}\right)^{(\lambda\mp\lambda')/2} e^J{}_{\lambda,\mp\lambda'}(z)dz=0. \tag{11}$$

With the above assumptions, the helicity amplitudes may be written as

$$(-1)^{\lambda'-\lambda}M_{\lambda\lambda'}(t,x)=-\pi\sum_{\substack{\text{Regge poles}\\ \mathrm{Re}\alpha>-\frac{1}{2}}}(\alpha+\tfrac{1}{2})\frac{\beta^{\pm}{}_{\lambda\lambda'}(t)}{\sin\pi(\alpha-\lambda)}d^{\pm}{}_{\lambda,-\lambda'}(-x,\alpha)-\sum_{J=0}^{\lambda'-1}(J+\tfrac{1}{2})A^J{}_{\lambda\lambda'}(t)d^J{}_{\lambda\lambda'}(x)$$

$$-\frac{1}{2i}\int_{-\frac{1}{2}-i\infty}^{-\frac{1}{2}+i\infty}\frac{dJ(J+\tfrac{1}{2})}{\sin\pi(J-\lambda)}[A^{+}{}_{\lambda\lambda'}(t,J)d^{+}{}_{\lambda,-\lambda'}(-x,J)+A^{-}{}_{\lambda\lambda'}(t,J)d^{-}{}_{\lambda,-\lambda'}(-x,J)]. \tag{12}$$

The region of interest is the high-energy region of the $s$ channel, which corresponds to large negative $x$ and small negative $t$. Since the representation (12) was proved valid only in the physical $t$-channel region, it must be continued to negative $t$. This can be done either by dispersion relations[14] or by using a slightly different representation for the partial-wave series.[15] The result is that the Regge-pole terms have the same form in the negative $t$ region, while the remaining terms are slightly different.

The representation (12) is suitable for continuation to large $x=\cos\theta$ also. As $x$ becomes large, $\cos\theta$ acquires an imaginary part which enters in the integral term of (12) as $\exp|\mathrm{Im}\theta||\mathrm{Re}J|$, and since $\mathrm{Re}J=-\frac{1}{2}$ and fixed, the integral converges independently of $\mathrm{Im}\theta$, or $x$. The large-$x$ behavior of the $d^J{}_{\lambda\lambda'}$ function is

$$d^J{}_{\lambda\lambda'}(x)\xrightarrow[|x|\to\infty]{} x^{|\mathrm{Re}J+\frac{1}{2}|-\frac{1}{2}}, \tag{13}$$

unless $J$ is real and satisfies $-\lambda'+\frac{1}{2}+|J+\frac{1}{2}|=-n$, in which case

$$d^J{}_{\lambda\lambda'}(x)\xrightarrow[|x|\to\infty]{} x^{-|J+\frac{1}{2}|-\frac{1}{2}}. \tag{14}$$

For the terms in (12), the Regge-pole terms are bounded by $x^{\mathrm{Re}\alpha}$, the integral term by $x^{-1/2}$, and the sum by $x^{-\lambda'}$, where $\lambda'\geq 1$. The Regge-pole terms will then dominate over the other terms for large values of $|x|$, with the terms with largest $\mathrm{Re}\alpha$ the most important.

An examination of (13) reveals why the contour integral was stopped at $\mathrm{Re}J=-\frac{1}{2}$, rather than at some more negative value. For $\mathrm{Re}J<-\frac{1}{2}$, we have

$$d^J{}_{\lambda\lambda'}(x)\xrightarrow[|x|\to\infty]{} x^{-\mathrm{Re}J},$$

which grows larger as $\mathrm{Re}J$ decreases. In this region, the integral term becomes more important and cannot be neglected compared to the Regge-pole terms, since $\mathrm{Re}\alpha>\mathrm{Re}J$. The point at which the integral term is bounded by the smallest power of $x$ is precisely at $\mathrm{Re}J=-\frac{1}{2}$. However, the values of some Regge trajectories are certainly less than zero in physical regions of interest, and the approximation of neglecting the integral term becomes worse and worse as $\alpha$ decreases, no matter what the value of $x$. Hence it is desirable to find a representation for the helicity amplitudes for which the Regge-pole terms will dominate for all values of $\alpha$. Such a method has been devised by Mandelstam[16] for spinless particles, subject to a symmetry property in $J$ of the partial-wave scattering amplitudes, which he proved for potential scattering. We propose to extend this method to particles with arbitrary spin.

We use the relation between the $e^J{}_{\lambda\lambda'}$ and $d^J{}_{\lambda\cdot}$ functions:

$$\frac{d^J{}_{\lambda\lambda'}(x)}{\sin\pi(J-\lambda)}=\frac{1}{\pi\cos\pi(J-\lambda)}\times[e^J{}_{\lambda\lambda'}(x)-e^{-J-1}{}_{-\lambda,-\lambda'}(x)]. \tag{15}$$

The $e^J{}_{\lambda\lambda'}(x)$ function has an asymptotic behavior of $x^{-J-1}$ for all $J$, so it is useful to use it rather than $d^J{}_{\lambda\lambda'}$ in the contour integral. We define a function $e^{\pm}{}_{\lambda\lambda'}(x,J)$ in an analogous manner to the $d^{\pm}{}_{\lambda\lambda'}(x,J)$. We start with (9) for the helicity amplitudes, and add and subtract the expression

$$\sum_{J=\lambda}^{\infty}\frac{J+1}{\pi}(-1)^{J-\lambda}\times[A^{\sigma}{}_{\lambda\lambda'}(t,J+\tfrac{1}{2})e^{\sigma}{}_{\lambda,-\lambda'}(-x,J+\tfrac{1}{2})], \tag{16}$$

[14] H. Cheng and R. Nunez-Lagos, Nuovo Cimento **26**, 177 (1962).

[15] A. Q. Sarker, Nuovo Cimento **30**, 1298 (1963).

[16] S. Mandelstam, Ann. Phys. (N. Y.) **19**, 254 (1962).

where a summation over $\sigma=\pm$ is implied. Using (15), we combine part of the sum with the original term in (9) and write the result as a contour integral:

$$(-1)^{\lambda'-\lambda}M_{\lambda\lambda'}(t,x)=\sum_{J=\lambda}^{N}(J+\tfrac{1}{2})A^{J}{}_{\lambda\lambda'}(t)d^{J}{}_{\lambda\lambda'}(x)+\sum_{J=\lambda}^{N}\frac{J+1}{\pi}(-1)^{J-\lambda}A^{\sigma}{}_{\lambda\lambda'}(t,J+\tfrac{1}{2})e^{\sigma}{}_{\lambda,-\lambda'}(-x,J+\tfrac{1}{2})$$

$$-\frac{1}{2\pi i}\int_{C}\frac{(J+\frac{1}{2})dJ}{\cos\pi(J-\lambda)}A^{\sigma}{}_{\lambda\lambda'}(t,J)e^{\sigma}{}_{-\lambda,\lambda'}(-x,-J-1)-\sum_{J=\lambda}^{\infty}\frac{J+1}{\pi}(-1)^{J-\lambda}A^{\sigma}{}_{\lambda\lambda'}(t,J+\tfrac{1}{2})e^{\sigma}{}_{\lambda,-\lambda'}(-x,J+\tfrac{1}{2}). \quad (17)$$

The contribution from the infinite semicircle again vanishes for $t\geq t_0$ and $-1\leq x\leq+1$. Now the contour at $\mathrm{Re}J=N+\frac{1}{2}$ is shifted to the left to $\mathrm{Re}J=L$, where we allow $L<-\frac{1}{2}$. We again assume that the only singularities of the $A^{\pm}{}_{\lambda\lambda'}(t,J)$ are Regge poles, and that the fixed poles due to the normalization factors of the rotation coefficients are cancelled by zeros in the continuation of the partial-wave amplitudes. The poles of $1/\cos\pi(J-\lambda)$ give terms at half-integer values of $J-\lambda$. Using

$$e^{J}{}_{\lambda\lambda'}(-z)=(-1)^{\lambda-\lambda'}e^{J}{}_{-\lambda,-\lambda'}(z), \quad (18)$$

we partially combine these terms with the subtracted summation (16) to obtain

$$(-1)^{\lambda'-\lambda}M_{\lambda\lambda'}(t,x)=\sum_{\mathrm{Re}\alpha>L}\frac{(\alpha+\frac{1}{2})}{\cos\pi(\alpha-\lambda)}\beta^{\pm}{}_{\lambda\lambda'}(t)e^{\pm}{}_{-\lambda,\lambda'}(-x,-\alpha-1)$$

$$+\frac{1}{2\pi i}\int_{L-i\infty}^{L+i\infty}\frac{dJ(J+\frac{1}{2})}{\cos\pi(J-\lambda)}A^{\sigma}{}_{\lambda\lambda'}(t,J)e^{\sigma}{}_{-\lambda,\lambda'}(-x,-J-1)$$

$$+\sum_{J=-\lambda-1}^{\lambda-1}\frac{(-1)^{J-\lambda'}}{\pi}(J+1)A^{\sigma}{}_{\lambda\lambda'}(t,-J-\tfrac{3}{2})e^{\pm\sigma}{}_{\lambda,-\lambda'}(-x,J+\tfrac{1}{2})$$

$$-\sum_{J=-N(L)-1/2}^{\infty}\frac{(-1)^{J-\lambda}}{\pi}(J+1)A^{\sigma}{}_{\lambda\lambda'}(t,J+\tfrac{1}{2})e^{\sigma}{}_{\lambda,-\lambda'}(-x,J+\tfrac{1}{2})$$

$$-\sum_{J=\lambda}^{-N(L)-\frac{3}{2}}\frac{(J+1)}{\pi}(-1)^{J-\lambda}\{e^{+}{}_{\lambda,-\lambda'}(-x,J+\tfrac{1}{2})[A^{+}{}_{\lambda\lambda'}(t,J+\tfrac{1}{2})-(-1)^{\lambda-\lambda'}A^{\pm}{}_{\lambda\lambda'}(t,-J-\tfrac{3}{2})]$$

$$+e^{-}{}_{\lambda,-\lambda'}(-x,J+\tfrac{1}{2})[A^{-}{}_{\lambda\lambda'}(t,J+\tfrac{1}{2})-(-1)^{\lambda-\lambda'}A^{\mp}{}_{\lambda\lambda'}(t,-J-\tfrac{3}{2})]\}, \quad (19)$$

where $N(L)$ is the smallest half-integer (or integer) greater than $L$ if $\lambda$ and $\lambda'$ are integer (or half-integer), and the upper and lower signs are for $\lambda$ and $\lambda'$ either integer or half-integer.

The last terms are zero if the partial-wave amplitudes are symmetric under the interchange $J\leftrightarrow-J-1$ for half-integer (unphysical) values of $J-\lambda$, which is obviously a generalization of the Mandelstam symmetry for potential scattering:

$$A^{\pm}{}_{\lambda\lambda'}(t,J+\tfrac{1}{2})=(-1)^{\lambda-\lambda'}\times\begin{cases}A^{\pm}{}_{\lambda\lambda'}(t,-J-\frac{3}{2}) & \text{for } J,\lambda,\lambda' \text{ integer}\\ A^{\mp}{}_{\lambda\lambda'}(t,-J-\frac{3}{2}) & \text{for } J,\lambda,\lambda' \text{ half-integer.}\end{cases} \quad (20)$$

If this is true, the first summation in (19) can be shown to be zero also. The final form for the helicity amplitudes is

$$(-1)^{\lambda'-\lambda}M_{\lambda\lambda'}(t,x)=\sum_{\mathrm{Re}\alpha>L}\frac{(\alpha+\frac{1}{2})}{\cos\pi(\alpha-\lambda)}\beta^{\pm}{}_{\lambda\lambda'}(t)e^{\pm}{}_{-\lambda,\lambda'}(-x,-\alpha-1)$$

$$+\frac{1}{2\pi i}\int_{L-i\infty}^{L+i\infty}\frac{dJ(J+\frac{1}{2})}{\cos\pi(J-\lambda)}A^{\sigma}{}_{\lambda\lambda'}(t,J)e^{\sigma}{}_{-\lambda,\lambda'}(-x,-J-1)$$

$$-\sum_{J=-N(L)-1/2}^{\infty}\frac{(J+1)}{\pi}(-1)^{J-\lambda}A^{\sigma}{}_{\lambda\lambda'}(t,J+\tfrac{1}{2})e^{\sigma}{}_{\lambda,-\lambda'}(-x,J+\tfrac{1}{2}). \quad (21)$$

Using the large-$J$ behavior of $A^{\pm}_{\lambda\lambda'}$ and $e^{\pm}_{\lambda\lambda'}$, we see that the infinite sum converges for $t \geq t_0$, independent of $x$, since $\mathrm{Im}J=0$ for all terms. The integral along the line $\mathrm{Re}J=L$ also converges independently of $x$, as did the previous integral for $L=-\frac{1}{2}$. Thus (21) is an appropriate form of the helicity amplitude to continue to large $x$.

The region of interest is $x \to -\infty$ with $t$ negative. The extension of (21) to negative $t$ will be assumed valid just as for (12). Here we examine the large-$x$ behavior. For $x$ real, the Regge-pole terms give a contribution proportional to $x^{\mathrm{Re}\alpha}$ for all $\alpha$. The integral term contains $e^{-J-1}$ for $\mathrm{Re}J=L$, so that it is bounded by $x^L$. The sum has terms which are bounded by $x^{-J-3/2}$, where $J$ takes on values $-N(L)-\frac{1}{2}$ to $\infty$. Since $N(L)$ is the largest half-integer (or integer) greater than $L$, the largest power of $x$ entering the sum will be less than $L$. Since the Regge-pole terms have $\mathrm{Re}\alpha > L$, they will dominate the amplitude for large $x$, even for negative values of $\mathrm{Re}\alpha$. The effect of moving the contour to the left is to cancel the part of the $d^J_{\lambda\lambda'}$ function which was proportional to $x^{-\mathrm{Re}J}$ for negative $\mathrm{Re}J$, provided that the generalized Mandelstam symmetry (20) is true.

In calculating cross sections from the helicity amplitudes, it is convenient to factor out a term which is independent of helicity. This is done by expressing the rotation coefficients in terms of hypergeometric functions and using various relations for their manipulation. The results are tabulated in the Appendix. Here we give the form of the result appropriate for $x$ real and less than $-1$, for integer helicities. If $\alpha<0$, we use (21) and write

$$\frac{e^{\pm}_{-\lambda,\lambda'}(-x,-\alpha-1)}{\cos\pi(\alpha-\lambda)} = -\pi\frac{[1\pm e^{-i\pi(\alpha-\lambda)}]}{2\sin\pi(\alpha-\lambda)} \times \frac{\Gamma(\alpha+\frac{1}{2})}{\pi^{1/2}\Gamma(\alpha+1)}(-2x)^{\alpha}F_{\lambda\lambda'}(\alpha,x), \quad (22)$$

where the helicity-dependent terms $F_{\lambda\lambda'}$ are expressed as polynomials in $1/x$ and $\alpha$, a hypergeometric function $F(-\alpha/2, (1-\alpha)/2, \frac{1}{2}-\alpha, 1/x^2)$, and its first derivative with respect to $1/x^2$. This form is convenient for high-energy approximations, since as $x \to -\infty$, $F_{\lambda\lambda'}$ approaches a constant, so that the only energy dependence left is contained in the $(-2x)^{\alpha}$ term. If $\alpha>0$, we use (12) and write again

$$\frac{-\pi d^{\pm}_{\lambda,-\lambda'}(-x,\alpha)}{\sin\pi(\alpha-\lambda)} = -\pi\frac{[1\pm e^{-i\pi(\alpha-\lambda)}]}{2\sin\pi(\alpha-\lambda)} \times \frac{\Gamma(\alpha+\frac{1}{2})}{\pi^{1/2}\Gamma(\alpha+1)}(-2x)^{\alpha}F_{\lambda\lambda'}(\alpha,x), \quad (23)$$

where now $F_{\lambda\lambda'}(\alpha,x)$ for $\alpha>0$ contains the same terms as for $\alpha<0$, but also some additional terms. These terms involve polynomials in $\alpha$ and $1/x$, plus the hypergeometric function $F(1+\alpha/2, \frac{1}{2}+\alpha, \alpha+\frac{3}{2}, 1/x^2)$ and its first derivative, all multiplied by a factor $\tan\pi\alpha(-2x)^{-2\alpha-1}$. It is this factor which makes (12) unsuitable for trajectory values less than $-\frac{1}{2}$, but for $\alpha>0$ it is a small correction as $x \to -\infty$. Using (22) or (23), the Regge-pole terms in the helicity amplitudes can be written in the same form for all $\alpha$, remembering that $F_{\lambda\lambda'}(\alpha,x)$ is defined differently for positive and negative $\alpha$:

$$M_{\lambda\lambda'}(t,x) = -\pi(-1)^{\lambda-\lambda'}\sum_{\text{Regge poles}}\frac{\Gamma(\alpha+\frac{3}{2})}{\pi^{1/2}\Gamma(\alpha+1)}\frac{[1\pm e^{-i\pi(\alpha-\lambda)}]}{2\sin\pi(\alpha-\lambda)} \times\beta^{\pm}_{\lambda\lambda'}(t)(-2x)^{\alpha(t)}F_{\lambda\lambda'}(\alpha,x). \quad (24)$$

There are two more simplifications to make before using the helicity amplitudes to calculate cross sections. One is to make the signature factor $[1\pm e^{-i\pi(\alpha-\lambda)}]/2\sin\pi(\alpha-\lambda)$ independent of helicity. For integer $\lambda$, it can be written as $[e^{-i\pi\alpha}\pm(-1)^{\lambda}]/2\sin\pi\alpha$. Recall that the functions $\beta^{\pm}_{\lambda\lambda'}(t)$ are residues of partial-wave amplitudes which were continued from even or odd values of $J-\lambda$. It is convenient to redefine these amplitudes so that the $\pm$ refers to continuation from even or odd $J$ values, independent of helicity. This is accomplished by leaving the definition as it is for even $\lambda$, but for odd $\lambda$, redefining $\beta^{\pm}_{\lambda\lambda'}(t) = -\beta^{\pm}_{\lambda\lambda'}(t)$. Then the signature factor and residue function can be written as $\beta^{\pm}_{\lambda\lambda'}(t)[1\pm e^{-i\pi\alpha}]/2\sin\pi\alpha$ for all helicities, where the $\pm$ now refers to Regge poles occurring in partial-wave amplitudes continued from even or odd values of $J$. Then the terms due to a given Regge trajectory with definite signature occur with the same factor in every helicity amplitude.

The second simplification involves absorbing the $t$ dependence of the factor $(-2x)^{\alpha}$ into the residue function. This will exhibit the energy dependence explicitly. We define new residue functions $R^{\pm}_{\lambda\lambda'}(t)$ by the equation

$$\beta^{\pm}_{\lambda\lambda'}(t) = \left[\frac{-k_t q_t}{(M_A M_B M_C M_D)^{1/2}}\right]^{\alpha} R^{\pm}_{\lambda\lambda'}(t), \quad (25)$$

where the square root of the product of the masses is an arbitrary but conventional scale factor. We can combine this factor with $x$ and write

$$2xk_t q_t = s - s_0(t), \quad (26)$$

where

$$s_0(t) = M_A^2 + M_B^2 - \frac{(t+M_A^2-M_C^2)(t+M_B^2-M_D^2)}{2t}. \quad (27)$$

The helicity amplitudes then become

$$M_{\lambda\lambda'}(t,x) = -\pi(-1)^{\lambda-\lambda'} \sum_{\text{Regge poles}} \frac{\Gamma(\alpha+\frac{3}{2})}{\pi^{1/2}\Gamma(\alpha+1)} \frac{1\pm e^{-i\pi\alpha}}{2\sin\pi\alpha} \times R^{\pm}_{\lambda\lambda'}(t) F_{\lambda\lambda'}(\alpha,x) \left(\frac{s-s_0(t)}{(M_A M_B M_C M_D)^{1/2}}\right)^{\alpha(t)}. \quad (28)$$

The amplitudes are now in a form suitable for the derivation of the differential cross section for the $s$-channel reaction. Trueman and Wick[17] have formulated crossing relations for helicity amplitudes. The crossing matrix involves products of rotation coefficients, but because of their orthogonality and completeness, they do not appear in the spin-averaged differential cross section. With the normalization factors included, the differential cross section can be written in terms of the $t$-channel helicity amplitudes as

$$\frac{d\sigma}{dt} = \frac{\prod_i (2M_i)}{16\pi[(s-M_A^2-M_B^2)^2-4M_A^2M_B^2]} \times \frac{1}{(2S_A+1)(2S_B+1)} \sum_{\lambda' s} |M_{\lambda_A\lambda_{\bar{C}},\lambda_{\bar{B}}\lambda_D}(t,x)|^2, \quad (29)$$

where the product of masses appears for fermions only, and $S_A$ and $S_B$ are the spins of initial particles $A$ and $B$.

If one Regge-pole term dominates the amplitude, we can use (28) and (29) and write the differential cross section as

$$\frac{d\sigma}{dt} = \frac{\prod_i (2M_i)}{64[(s-M_A^2-M_B^2)^2-4M_A^2M_B^2]} \times \left(\frac{\Gamma(\alpha+\frac{3}{2})}{\Gamma(\alpha+1)}\right)^2 \left[1+\begin{pmatrix}\cot^2\\ \tan^2\end{pmatrix}\tfrac{1}{2}\pi\alpha\right] \times \left(\frac{s-s_0(t)}{(M_A M_B M_C M_D)^{1/2}}\right)^{2\alpha(t)} \frac{1}{(2S_A+1)(2S_B+1)} \times \sum_{\lambda' s} |(-1)^{\lambda-\lambda'} R^{\pm}_{\lambda\lambda'}(t) F_{\lambda\lambda'}(\alpha,x)|^2, \quad (30)$$

where $\cot^2$ or $\tan^2$ is used for even or odd signature, and we must remember that the $\lambda\lambda'$ indices on the residue functions actually indicate dependence on the individual particle helicities, $\lambda_A\lambda_{\bar{B}}\lambda_{\bar{C}}\lambda_D$.

We can examine the high-energy limit of the cross section from (30). This region is reached by letting $s\to\infty$, $x\to-\infty$, $t$ finite and negative. From the Appendix, we see that as $x\to-\infty$, the functions $F_{\lambda\lambda'}$ become approximately independent of $x$, and only depend on $t$, through their $\alpha$ dependence. We can then combine all of the $t$-dependent factors into one function $G(t)$, and write

$$\frac{d\sigma}{dt} \xrightarrow[s\to\infty]{} \frac{G(t)}{(s-M_A^2-M_B^2)^2-4M_A^2M_B^2} \times \left(\frac{s-s_0(t)}{(M_A M_B M_C M_D)^{1/2}}\right)^{2\alpha(t)}. \quad (31)$$

The energy dependence of the differential cross section is determined by the trajectory value $\alpha(t)$ in the high-energy limit. The validity of the one-Regge-pole approximation can be checked and the trajectory values can be determined from the experimental values of $d\sigma/dt$.

The single-pole formula (31) predicts that the dependence of $\ln\{[(s-M_A^2-M_B^2)^2-4M_A^2M_B^2]d\sigma/dt\}$ on $\ln[s-s_0(t)]$ at constant $t$ should be linear with a slope $2\alpha(t)$. This method will be used in the next section to check the Regge-pole hypothesis and determine trajectory values for some resonance production reactions. However, it must be remembered that (31) holds only in the limiting case where $|x|$ is sufficiently large to allow the energy dependence of the $F_{\lambda\lambda'}$ functions to be neglected. Calculations for various reactions show that for the presently available energies most of the $x$ values for resonance production reactions are not large. Also, $|x|=1$ in the forward direction for all resonance production reactions, independent of energy, so that there is a region around the forward direction which must be excluded from consideration if the approximate formula (31) is to be used. For these reasons, the exact form (30) must be used in most applications.

There have been some objections to using the Regge-pole formula when $x$ is not large.[18] The argument is that when $x$ is not large enough to use high-energy approximations, then it is not valid to assume the dominance of the Regge pole with the largest trajectory value over other Regge-pole terms and the background integral. However, it has become obvious that even in elastic scattering, where the high-energy approximations are certainly valid for the individual Regge-pole terms, all known poles must be included to get reasonable agreement with experiment at the presently available energies. We therefore do not assume the dominance of one pole in the resonance production reactions, but consider contributions from all poles which may be exchanged. A simplification occurs, since conservation laws (isospin, $G$ parity, parity, strangeness, etc.) limit the number of poles which can be exchanged, and for resonance production reactions, this sometimes reduces the number of poles to just one or two. As for the background integral, if we assume the generalized Mandelstam symmetry (20), the contour integral may be pushed as far to the left as desired in the complex $J$ plane. Then, its contribution may be made as small as

[17] T. L. Trueman and G. C. Wick, Ann. Phys. (N. Y.) **26**, 322 (1964).

[18] V. Barger and D. Atkinson, Nuovo Cimento **38**, 634 (1965).

desired for any $|x|>1$, if all Regge poles inside this larger contour are included.

Recently, Freedman and Wang[19] have resolved the problem of the Regge expansion for backward scattering of unequal-mass particles, in which the cosine of the crossed-channel scattering angle is bounded by unity for all energies. They found that the correct expression is given by the leading term alone, proportional to $s^\alpha$, and that the remaining terms are cancelled by contributions from a family of "daughter trajectories," whose zero intercepts occur at $\alpha(0)-1$, $\alpha(0)-2$, etc. A natural extension of this idea to helicity amplitudes is to retain the kinematic factors $[(1\pm x)/2]^{(\lambda\pm\lambda')/2}$, but replace the hypergeometric function in the $d^\alpha_{\lambda\lambda'}(x)$ by the leading term, proportional to $s^{\alpha-\lambda}$. This still has the $s^\alpha$ dependence in the limit of large $x$, but for small $x$ it will differ from the exact form of (30). However, for the reactions considered here, this difference is not very significant. It will be discussed along with the individual reactions.

When the exact form (30) for the cross section is used, the determination of the trajectory values from experiment is not as easy as before, since now there is additional energy dependence in the $F_{\lambda\lambda'}$ functions. Each of these functions is multiplied by an unknown residue function $R_{\lambda\lambda'}(t)$, so that for the energy dependence to be known, the relative magnitudes of the residue functions for different helicity values must be determined. The relative magnitudes of the residue functions for different helicities determine the state of polarization of the final particles, and this polarization is measured in resonance production by observing the angular distribution of the decay products. The experimentally determined quantities are the elements of the spin density matrix for the resonance, $\rho_{mm'}$.

The useful relation for Regge-pole applications was derived by Gottfried and Jackson,[20] who found that if the spin density matrix is measured in the rest frame of the produced resonance, it can be simply expressed in terms of the helicity amplitudes for the crossed-channel reaction. If the resonance is particle $C$, then the connection is

$$\rho_{mm'}=\frac{\sum_{\lambda_A\lambda_{\bar B}\lambda_D} M_{\lambda_{\bar B}\lambda_D,\lambda_A m}{}^* M_{\lambda_{\bar B}\lambda_D,\lambda_A m'}}{\sum_{\lambda_A\lambda_{\bar B}\lambda_{\bar C}\lambda_D}|M_{\lambda_{\bar B}\lambda_D,\lambda_A\lambda_{\bar C}}|^2}. \tag{32}$$

From this, we can see that the diagonal elements $\rho_{mm}$ give the fractional contribution of certain helicity amplitudes to the differential cross section. The experimental values are used to determine the ratios of the residue functions, and the energy dependence of the differential cross section then only depends on the trajectory value. Note that the density matrix value is needed only at one energy, since the residue functions are independent of energy. Once they are fixed and the trajectory values determined from the differential cross section, the energy dependence of the spin density matrix elements is predicted.

The actual method used to determine the trajectory values from experiment is the same as in the case where the approximate form was valid, except for the complications arising from the $\alpha$ dependence of the $F_{\lambda\lambda'}$ functions. To get around this, an iteration technique is used, in which $\alpha$ is first determined from the approximate formula (31). This value is then used in the $F_{\lambda\lambda'}$ function, and a new value is determined from the energy variation of the differential cross section due to the $(-2x)^\alpha$ factor. This new value is used in the $F_{\lambda\lambda'}$ function, and the procedure repeated until the trajectory values converge. Since the main energy variation is in the $(-2x)^\alpha$ factor, and the $F_{\lambda\lambda'}$ functions are corrections for small $x$, this procedure converges rapidly, usually requiring less than ten iterations for a 1% agreement between input and output trajectory values.

## III. COMPARISON WITH EXPERIMENTS

### Baryon Resonance Production

The best known baryon resonance is the "3–3" pion-nucleon resonance $N^*(1238)$. It is produced in a large fraction of the single-pion production events in $\pi$ and $K$ meson-nucleon reactions with lab momentum from 2–8 GeV/$c$:

$$\pi^+ + p \to \pi^0 + N^{*++}, \tag{33a}$$

$$K^+ + p \to K^0 + N^{*++}. \tag{33b}$$

The distribution of the $\pi^0$ or $K^0$ is peaked in the forward direction, indicating the dominance of a peripheral interaction. We examine the crossed-channel reaction to determine what particles might be exchanged:

$$\pi^+(K^+) + \pi^0(\bar K^0) \to \bar p + N^{*++}. \tag{34}$$

For reaction (33a), we note that the $\pi^+\pi^0$ system has isospin $I=0$, 1, or 2, zero baryon number and strangeness, and positive $G$ parity. The $K^+\bar K^0$ system has isospin $I=0$ or 1, zero baryon number and strangeness, but arbitrary $G$ parity. The $\bar pN^*$ system has isospin $I=1$ or 2, which rules out isospin zero exchange.

For parity considerations, we write the helicity state of the $\bar pN$ system as $|J\lambda_1\lambda_2\rangle$, where $\lambda_1$ is the $\bar p$ helicity ($\pm\frac{1}{2}$) and $\lambda_2$ is the $N^*$ helicity ($\pm\frac{1}{2}$, $\frac{3}{2}$). From the Appendix, we see that the parity operation produces

$$\begin{aligned} P|J\lambda_1\lambda_2\rangle &= P_{\bar p}P_{N^*}(-1)^{J-S_{\bar p}-S_{N^*}}|J-\lambda_1-\lambda_2\rangle \\ &= -(-1)^J|J-\lambda_1-\lambda_2\rangle. \end{aligned} \tag{35}$$

For the two-pion or two-kaon states, all helicities are zero, so that

$$P|2\pi\rangle=(-1)^J|2\pi\rangle, \tag{36a}$$

$$P|K\bar K\rangle=(-1)^J|K\bar K\rangle, \tag{36b}$$

[19] D. Z. Freedman and J.-M. Wang, Phys. Rev. Letters **17**, 569 (1966).

[20] K. Gottfried and J. D. Jackson, Nuovo Cimento **33**, 309 (1964).

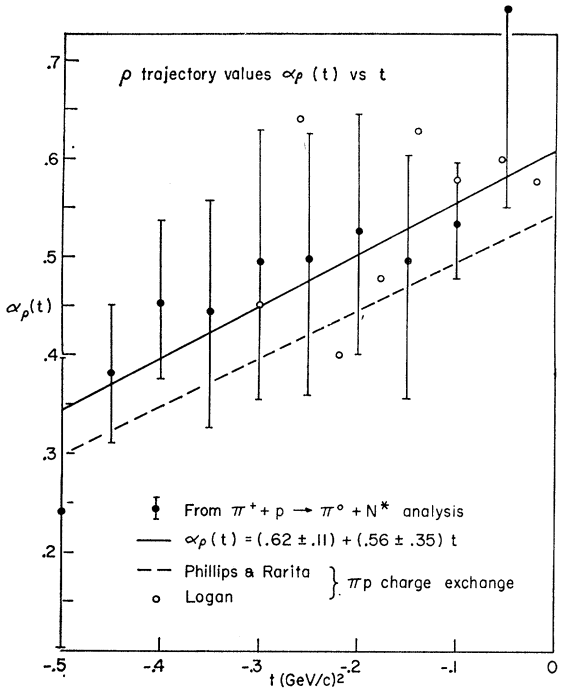


FIG. 1. $\rho$ trajectory values.

and if parity is to be conserved, the intermediate particle must have parity $P=(-1)^J$. If we denote the $t$-channel helicity amplitudes by $\langle\lambda_1\lambda_2|M^J|i\rangle$, where $i$ is the initial $2\pi$ or $K\bar{K}$ state, parity conservation requires

$$\langle\lambda_1\lambda_2|M^J|i\rangle=-\langle-\lambda_1-\lambda_2|M^J|i\rangle. \quad (37)$$

This reduces the number of independent amplitudes from 8 to 4.

The exchanged particle must have quantum numbers $I=1$ (or 2), $B=S=0$, $P=(-1)^J$, and $G=+1$ for reaction (33a). Among the well-known particles, only the $\rho$ meson satisfies these restrictions. For reaction (33b), the $G$ parity can either be $+$ or $-$. From the Appendix, for the $K\bar{K}$ state to couple to a particle and conserve $G$ parity, we must have $G=(-1)^{I+J}$. This is satisfied by the $\rho$ and also the $A_2$ resonance, which is presumed to lie on the $R$ trajectory.

Assume now that the partial-wave helicity amplitudes have poles at the positions of these trajectories, and denote the residues by $R_{2\lambda_1,2\lambda_2}(t)$. For reaction (33a), only the $\rho$ is exchanged, so we have

$$\frac{d\sigma}{dt}=\frac{MM^*}{16[(s-M^2-\mu^2)^2-4M^2\mu^2]}\times\left(\frac{\Gamma(\alpha_\rho+\tfrac{1}{2})}{\Gamma(\alpha_\rho+1)}\right)^2[1+\tan^2(\pi\alpha_\rho/2)]\times\left(\frac{s-\mu^2-\tfrac{1}{2}(M^2+M^{*2}-t)}{\mu(MM^*)^{1/2}}\right)^{2\alpha_\rho(t)}N_\rho, \quad (38)$$

where

$$N_\rho=R_{11}^2|F_{00}|^2+(R_{1,-1}^2+R_{13}^2)|F_{10}|^2+R_{1,-3}^2|F_{20}|^2. \quad (39)$$

In these formulas, $M$ is the nucleon mass, $\mu$ the pion mass, $M^*$ the $N^*$ mass, $\alpha_\rho(t)$ the $\rho$ trajectory value, and the $F_{\lambda\lambda'}$ are functions of $\alpha_\rho$ and $z$ defined in the Appendix.

The spin density matrix elements for the $N^*$ decay are

$$\rho_{33}=\frac{\frac{1}{2}R_{13}^2|F_{10}|^2+\frac{1}{2}R_{1,-3}^2|F_{20}|^2}{N_\rho}, \quad (40)$$

$$\mathrm{Re}\rho_{3,-1}=\frac{-\frac{1}{2}R_{13}R_{1,-1}|F_{10}|^2+\frac{1}{2}R_{1,-3}R_{11}|F_{20}||F_{00}|}{N_\rho}, \quad (41)$$

$$\mathrm{Re}\rho_{31}=\frac{-\frac{1}{2}R_{13}R_{11}Re(F_{10}^*F_{00})-\frac{1}{2}R_{1,-3}R_{1,-1}Re(F_{10}^*F_{20})}{N_\rho}. \quad (42)$$

Data on reaction (33a) exist at pion lab momenta of 1.6,[21] 2.75,[22] 3.5,[23] 4.0,[24] and 8.0[25] GeV/$c$. Analysis of the values of the cosine of the $t$-channel scattering angle for this reaction shows that the functions are independent of $z$ to a good approximation. Then the function $N_\rho$ is only a function of $t$, and a simple analysis to test the Regge-pole hypothesis is possible.

From (38), we see that the dependence of $\ln[(s-M^2-\mu^2)^2-4M^2\mu^2]$ on $\ln[s-\mu^2-\frac{1}{2}(M^2+M^{*2}-t)]$ at constant $t$ should be linear with a slope of $2\alpha_\rho(t)$. This method was applied to the data, and the trajectory values found by the least-squares fit of a straight line. The linear formula was found to fit the data at all energies except the lowest (1.6 GeV/$c$), which evidently is too low for the Regge-pole theory to be valid. The trajectory values were determined as a function of $t$

[21] A. Daudin, M. A. Jabriol, C. Kochowski, C. Lewin, S. Mongelli, A. Romano, and P. Waloschek, Phys. Letters 7, 125 (1963).
[22] Saclay-Orsay-Bari-Bologna Collaboration, Phys. Letters 13, 341 (1964).
[23] M. Abolins, D. Carmony, D. N. Hoa, R. L. Lander, C. Rindgfleisch, and N. H. Xuong, Phys. Rev. 136, B195 (1964).
[24] German-British Collaboration, Nuovo Cimento 34, 495 (1964).
[25] Aachen-Berlin-CERN Collaboration, Phys. Letters 19, 608 (1965); D. R. O. Morrison and S. Nowak (private communication).

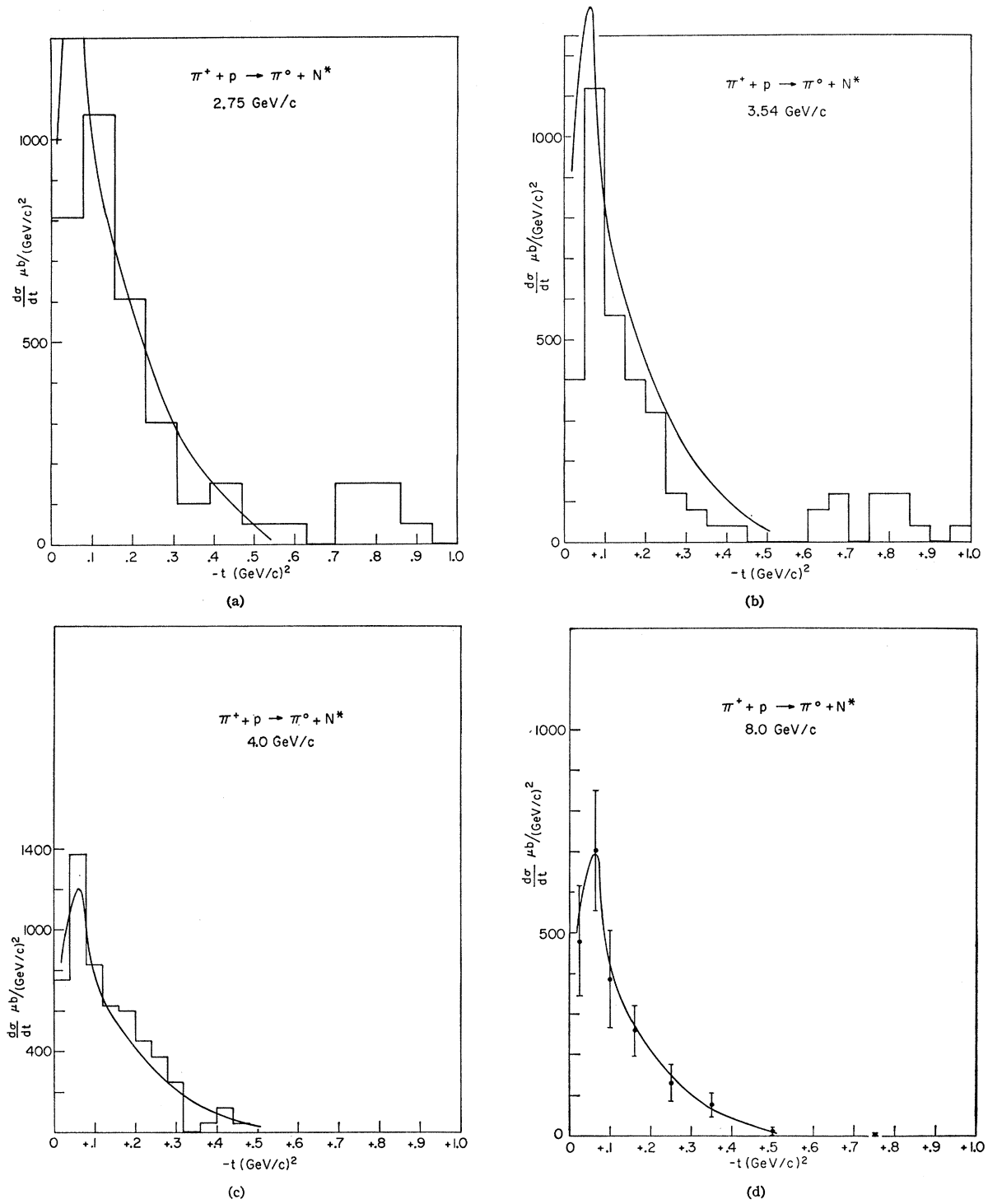


FIG. 2. Differential cross sections for the reaction $\pi^+ + p \rightarrow \pi^0 + N^*$.

for $-0.5 \leq t \leq -0.05$ $(\mathrm{GeV}/c)^2$, and the results are shown in Fig. 1. The error bars were computed from the statistical uncertainty of a straight-line fit to the data, and do not take into account possible errors in the data itself. The trajectory can be parameterized by a linear formula,

$$\alpha_\rho(t) = 0.62 \pm 0.11 + (0.56 \pm 0.35)t. \quad (43)$$

The $\rho$ trajectory values have also been determined from an analysis of $\pi p$ charge-exchange scattering, and

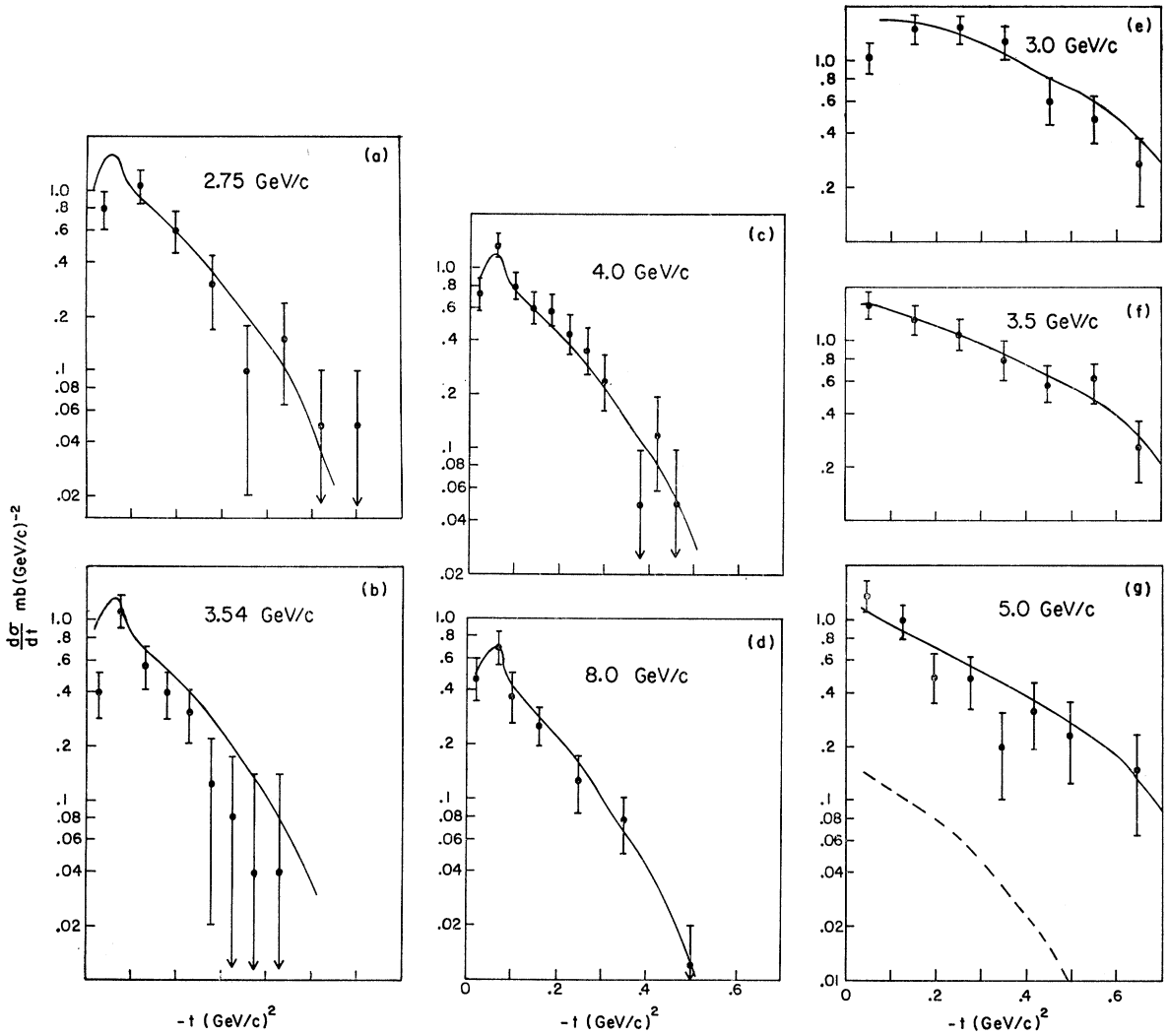


FIG. 3. Differential cross section for (a)–(d): $\pi^+ + p \to \pi^0 + N^*$; (e)–(g): $K^+ + p \to K^0 + N^*$.

the results of Phillips and Rarita[1] and Logan[3] are shown in Fig. 1 for comparison. It is seen that the trajectory values agree quite well. However, the more recent results of Höhler *et al.*[4] indicate that the slope of the $\rho$ trajectory is larger. Their linear fit gives $\alpha_\rho(t) = 0.57 + 0.91t$, which agrees with the $N^*$ results in the small $t$ region but disagrees for $-t > 0.3$ (GeV/$c$)$^2$. This difference can be reconciled by including the statistical errors for the $N^*$ production data in the error limits for the trajectory values. Since the data points for this $t$ region are due to events which number typically less than ten [see Figs. 2 and 3(a)], the error limits on the trajectory values can be expanded enough to be compatible with the new charge-exchange results.

The unknown function of $t$, $N_\rho$, is determined by fitting the angular distribution at 8.0 GeV/$c$. Within experimental errors, it is found to be consistent with a constant, for $-t > 0.05$ (GeV/$c$)$^2$:

$$N_\rho(t) = 2.3 \pm 0.3 \text{ mb}. \quad (44)$$

The observed dip in the forward direction requires a decrease in the residue function. However, in this region the asymptotic form of the $F_{\lambda\lambda'}$ function is not valid. From (39) and the Appendix, we see that three of the four independent helicity amplitudes vanish in the forward direction, so that a minimum in this region can easily be produced with constant residue functions. These same three amplitudes also vanish when the trajectory value is zero, and should produce another minimum at this point.[5,26] There is some evidence of this minimum for the low-energy data at $t \approx -0.5$ (GeV/$c$)$^2$, which is in the region where the $\rho$ trajectory seems to go through zero.

The calculated differential cross section is compared with the data in Fig. 2, and again on a logarithmic scale with the experimental errors indicated in Fig. 3(a). It is seen that the calculated values are within the experimental error limits for all cases, with the worst fit

[26] L.-L. Wang, Phys. Rev. Letters **16**, 756 (1966).

being at 3.5 GeV/$c$, where they are consistently higher than the data points. This is due to the relative dip in the production cross section at this energy. The reported value is 0.20±0.04 mb, compared with the 2.75 GeV/$c$ value of 0.30±0.03 mb and the 0.29±0.03 mb value at 4.0 GeV/$c$. If the cross section actually does have this structure, rather than decreasing with increasing energy everywhere, a one-Regge-pole fit with its smooth $s^{2\alpha-2}$ energy variation cannot be expected to fit the curve. However, this dip could easily be due merely to a systematic difference in normalization for the different experiments, and more accurate data are necessary to determine the precise energy variation of the cross section.

The individual residue functions must be determined in order to calculate the spin density matrix elements. However, since $F_{10}$ is imaginary and $F_{00}$ and $F_{20}$ real, (42) reduces to

$$\mathrm{Re}\rho_{31}=0. \tag{45}$$

This property is not a unique prediction of Regge-pole exchange, but depends only on parity conservation and the fact that all helicity amplitudes have the same phase, which is true only for a single trajectory exchange. Combining (40) and (41) leads to the restriction

$$(\mathrm{Re}\rho_{3,-1})^2\leq\tfrac{1}{2}\rho_{33}(1-2\rho_{33})/2. \tag{46}$$

Data at 4 and 8 GeV/$c$ indicate that $\mathrm{Re}\rho_{31}=0\pm0.15$, $\rho_{33}=0.2-0.4$, and $\mathrm{Re}\rho_{3,-1}=0-0.2$, so that (45) and (46) are satisfied. The energy variation is the only unique prediction of the Regge theory. For this reaction, the functions $F_{\lambda\lambda'}$ are approximately independent of energy, so that the $\rho_{mm'}$ are predicted to be energy-independent also, which is in agreement with the limited data available.[27]

For the reaction (33b), the differential cross section and spin density matrix elements are given by the same formulas as for reaction (33a) for a single Regge trajectory exchange, but if two trajectories are exchanged, the interference term must also be considered. Data on this reaction exist at lab momenta of 1.96,[28] 3.0,[29] 3.5,[30] and 5.0[30] GeV/$c$. Examination of the kinematics reveals that the $F_{\lambda\lambda'}$ functions are approximately independent of energy in this reaction for lab momentum greater than 3 GeV/$c$ and for $t<-0.1$ (GeV/$c$)$^2$. A one-pole analysis was tried for data from the highest three energies. A fairly good fit was obtained, but the trajectory values did not agree with the $\rho$ values, starting at about the same value in the forward direction, but decreasing with $t$ much faster. The $\rho$ trajectory

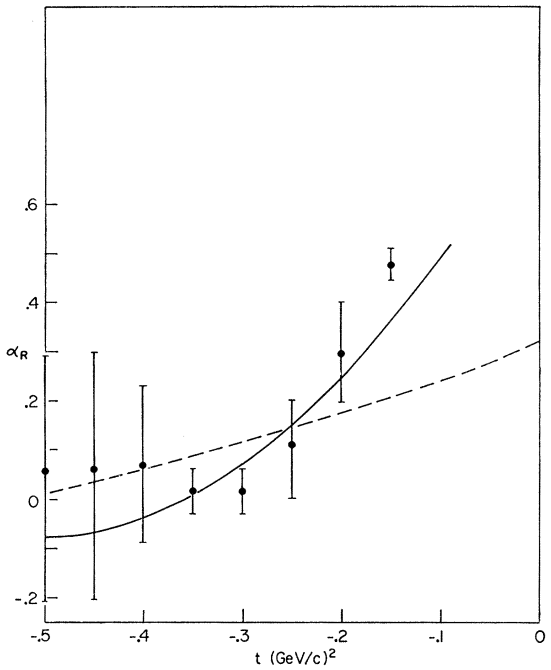


FIG. 4. $A_2$ trajectory values $\alpha_R(t)$ versus $t$: Data points taken from $K^+ + p \to K^0 + N^*$ analysis. Solid line: $\alpha_R(t)=0.80+3.5t+3.5t^2$; dashed line: Philips and Rarita, $Kp$ elastic and charge exchange.

exchange alone cannot explain reaction (33b), and $A_2$ exchange must also be considered.

A partial separation of the two contributions may be accomplished if we assume $SU(3)$ symmetry for the $\rho\pi\pi$ and $\rho KK$ couplings. In order to preserve charge conjugation invariance, the coupling of the $\rho$ octet to the $\pi\pi$ and $KK$ octets must be pure $F$ type.[31] Then there is a unique relation between the coupling strengths:

$$g_{\rho\pi\pi}{}^2=2g_{\rho KK}{}^2. \tag{47}$$

The residue functions for $\rho$ exchange in reaction (33b) can then be calculated from those determined for (33a). The squared term in the cross section was calculated from $N_\rho(t)$, and found to contribute only 2 to 20% of the experimental cross section. The smallness is due in part to the factor of 2 in (47), and the remainder to the difference in $\cos\theta$ values arising from the $\pi$-$K$ mass difference.

The interference term depends on products of individual residue functions, and hence cannot be calculated directly. An upper limit can be calculated, using the Schwarz inequality and the phase difference of the amplitudes. Since the $\rho$ and $A_2$ trajectories have opposite signature, the interference term will be proportional to

$$\mathrm{Re}(1-e^{+i\pi\alpha_\rho})(1+e^{-i\pi\alpha_R})\sim\sin(\pi\Delta\alpha/2), \tag{48}$$

where $\Delta\alpha=\alpha_\rho-\alpha_R$. Using the trajectory value of the $A_2$ from charge-exchange scattering, the interference

[27] N. Schmitz, CERN Report No. 65-24, Vol. I (unpublished).
[28] S. Goldhaber, *Athens Topical Conference on Recently Discovered Resonant Particles*, edited by B. A. Munirt, and L. S. Gallagher (Ohio University Press, Athens, Ohio, 1963), p. 92.
[29] M. Ferro-Luzzi, R. George, Y. Goldschmidt-Clermont, V. P. Henri, B. Jongejans, D. W. G. Leith, G. R. Lynch, F. Muller, and J. M. Perreau, Nuovo Cimento **36**, 1101 (1965).
[30] Preliminary data on $K^+p$ interactions at 3.5 and 5.0 GeV/$c$. Y. Goldschmidt-Clermont (private communication).
[31] H. Lipkin, Phys. Letters **7**, 221 (1963).

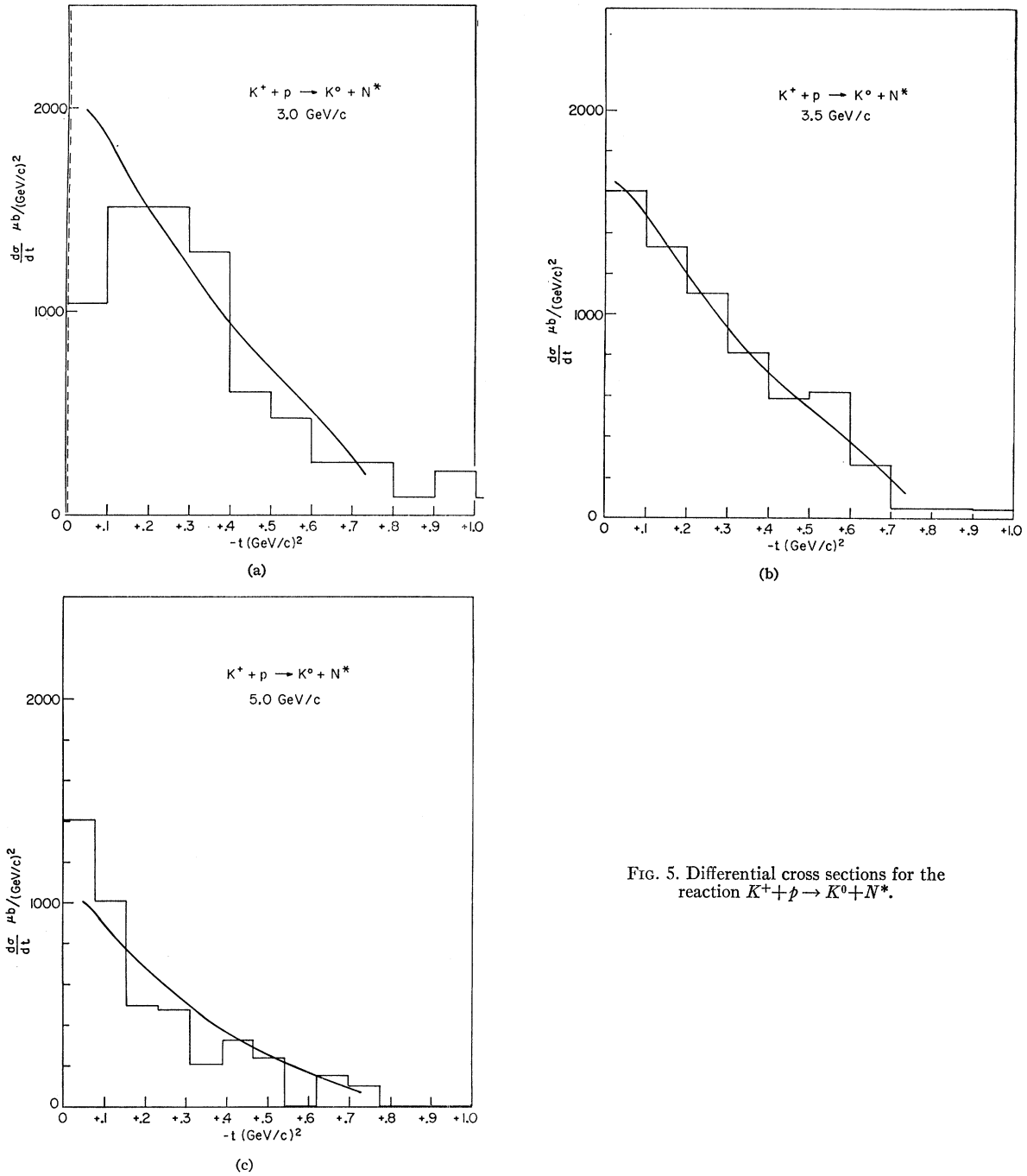


FIG. 5. Differential cross sections for the reaction $K^+ + p \rightarrow K^0 + N^*$.

term was estimated, resulting in an upper limit of 15% of the experimental cross section. Thus if Regge-pole exchange is to explain reaction (33b), the main contribution must come from the $R$ trajectory.

The single-pole analysis was redone, with the contribution from $\rho$ exchange subtracted out and the interference term neglected, and again a fairly good fit obtained. The trajectory values are shown in Fig. 4, along with the $R$ trajectory from charge-exchange scattering.[1] The two agree quite well, except at small momentum transfer. In this region, however, the $z$ values are the smallest, and the high-energy approximation the least accurate. The sum of the squares of the residue functions $N_R(t)$ [the analog of $N_\rho$ for reaction (33a)], was determined by fitting the angular distribution at 3.5 GeV/$c$. It has a sharp minimum around $t=-0.35$ (GeV/$c$)$^2$. This is due to the "ghost" pole of the even-signature $R$ trajectory at $\alpha=0$, which must be

compensated by the vanishing of the residue function at this point. The function $N_R'(t)=N_R(t)/(\alpha_R(t))^2$ is a much more slowly varying function:

$$N_R'(t)=(5.0\pm0.3)\times10^3-(9.1\pm0.9)\times10^3 t \text{ mb}. \quad (49)$$

The calculated differential cross sections are compared with the data in Fig. 5, and again on a logarithmic scale with error bars on the data in Fig. 3(b). The calculated values fit the data within errors, except at the lowest energy and at low momentum transfer as expected, where the approximate Regge formula is not valid. It is seen that the disagreement of the trajectory values at low momentum transfer is caused by the flattening of the 3.0-GeV/$c$ differential cross section in the forward direction, which makes the trajectory values rise rapidly. It is possible that this effect is due merely to the high-energy approximation, but without the knowledge of the individual residue functions, an exact calculation cannot be performed. A determination of the forward differential cross section at higher energies is necessary to resolve this point.

The relations for the spin density matrix elements (45) and (46) are now only approximate, since with two-trajectory exchange, the phases of the individual residue functions vary with the relative contribution of each trajectory. However, the limited data available[27] are consistent with these restrictions.

### Meson Resonance Production

Here we consider the production of the $2\pi$ resonances $\rho$ and $f^0$ by pion-nucleon interactions. The $f^0$ is produced in the equivalent reactions

$$\pi^-+p\rightarrow f^0+n, \quad (50a)$$

and

$$\pi^++n\rightarrow f^0+p. \quad (50b)$$

In the crossed reaction, $\pi+f\rightarrow\bar{p}+n$, the intermediate particle must have isospin $I=1$, negative $G$ parity, and zero strangeness and baryon number. Of the known mesons, only the $A_2$ and the $\pi$ (also the $A_1$ if it exists) have these quantum numbers.

Let the $\pi f$ state be represented by $|\beta\rangle$, where $\beta$ is the helicity of the $f$, and the $\bar{p}n$ state represented by $|\lambda_1\lambda_2\rangle$, where $\lambda_1$ is the $\bar{p}$ helicity and $\lambda_2$ the $n$ helicity. Then the requirement of parity conservation for the $t$-channel helicity amplitudes asserts

$$\langle\lambda_1\lambda_2|M^J|\beta\rangle=-\langle-\lambda_1-\lambda_2|M^J|-\beta\rangle. \quad (51)$$

If we further specialize to intermediate states with parity $P=(-1)^J$ (the $R$ trajectory), we have

$$\langle\lambda_1\lambda_2|M^J|\beta\rangle=-\langle\lambda_1\lambda_2|M^J|-\beta\rangle, \quad (52)$$

which means that all $\beta=0$ amplitudes are zero. From the Appendix, we see that $G$ parity conservation at the $\bar{p}$ $n$ vertex brings in no additional restrictions.

For the other case, $P=-(-1)^J$, and we have

$$\langle\lambda_1\lambda_2|M^J|\beta\rangle=\langle\lambda_1\lambda_2|M^J|-\beta\rangle. \quad (53)$$

From the Appendix, we see that $G$ parity conservation at the $\bar{p}$ $n$ vertex requires that for even $J$ values ($\pi$ trajectory)

$$\langle\tfrac{1}{2}\tfrac{1}{2}|M^J|\beta\rangle=-\langle-\tfrac{1}{2},-\tfrac{1}{2}|M^J|\beta\rangle, \quad (54)$$
$$\langle\tfrac{1}{2},-\tfrac{1}{2}|M^J|\beta\rangle=\langle-\tfrac{1}{2},\tfrac{1}{2}|M^J|\beta\rangle=0,$$

and for odd $J$ values ($A_1$ trajectory?)

$$\langle\tfrac{1}{2},-\tfrac{1}{2}|M^J|\beta\rangle=-\langle-\tfrac{1}{2},\tfrac{1}{2}|M^J|\beta\rangle, \quad (55)$$
$$\langle\tfrac{1}{2}\tfrac{1}{2}|M^J|\beta\rangle=\langle-\tfrac{1}{2},-\tfrac{1}{2}|M^J|\beta\rangle=0.$$

For these cases, the requirements of parity and $G$ parity conservation reduce the number of independent helicity amplitudes from 20 to 3.

We can write the differential cross section and spin density matrix elements for Regge-pole exchange in terms of the trajectory values and the residue functions for the helicity amplitudes, which we denote by $R_{\beta,2\lambda_1 2\lambda_2}(t)$. There are three cases to consider.

*(a) $\pi$ Trajectory Exchange*

$$\frac{d\sigma}{dt}=\frac{M^2}{8[(s-M^2-\mu^2)^2-4M^2\mu^2]}\times\left(\frac{\Gamma(\alpha+\frac{3}{2})}{\Gamma(\alpha+1)}\right)^2[1+\cot^2(\pi\alpha/2)]\times\left(\frac{s-M^2-\frac{1}{2}(\mu^2+m_f{}^2-t)}{M(\mu m_f)^{1/2}}\right)^{2\alpha_\pi(t)}N_\pi, \quad (56)$$

$$N_\pi=R_{2,11}{}^2|F_{20}|^2+R_{1,11}{}^2|F_{10}|^2+\tfrac{1}{2}R_{0,11}{}^2|F_{00}|^2, \quad (57)$$

$$\rho_{00}=\tfrac{1}{2}R_{0,11}{}^2|F_{00}|^2/N_\pi, \quad (58a)$$

$$\rho_{11}=\tfrac{1}{2}R_{1,11}{}^2|F_{10}|^2/N_\pi, \quad (58b)$$

$$\rho_{22}=\tfrac{1}{2}(1-2\rho_{11}-\rho_{00}), \quad (58c)$$

$$\rho_{1,-1}=-\rho_{11}, \quad (58d)$$

$$\mathrm{Re}\rho_{10}=\tfrac{1}{2}R_{1,11}{}^2R_{0,11}{}^2\,\mathrm{Re}(F_{10}{}^*F_{00})/N_\pi. \quad (58e)$$

*(b) $A_1$ Trajectory Exchange*

$$\frac{d\sigma}{dt}=\frac{M^2}{8[(s-M^2-\mu^2)^2-4M^2\mu^2]}\times\left(\frac{\Gamma(\alpha+\frac{3}{2})}{\Gamma(\alpha+1)}\right)^2[1+\tan^2(\pi\alpha/2)]\times\left(\frac{s-M^2-\frac{1}{2}(\mu^2+m_f{}^2-t)}{M(\mu m_f)^{1/2}}\right)^{2\alpha_{A1}(t)}N_A, \quad (59)$$

$$N_A=\tfrac{1}{2}R_{2,1-1}{}^2(|F_{2,-1}|^2+|F_{21}|^2)+\tfrac{1}{2}R_{0,11}{}^2|F_{10}|^2+\tfrac{1}{2}R_{1,1-1}{}^2(|F_{1,-1}|^2+|F_{11}|^2), \quad (60)$$

$$\rho_{00}=\tfrac{1}{2}R_{0,1-1}{}^2|F_{10}|^2/N_A, \quad (61a)$$

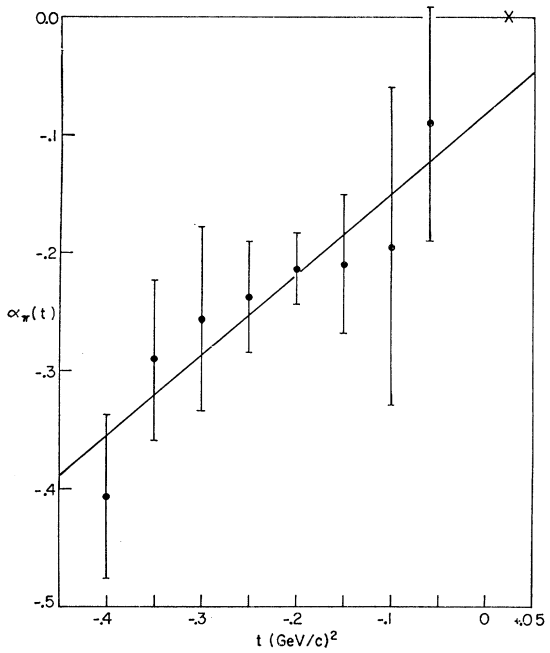


FIG. 6. Pi trajectory values $\alpha_\pi(t)$ versus $t$, from $\pi^-+p\to f^0+n$ analysis, $\alpha_\pi(t)=-0.08\pm0.07+(0.69\pm0.29)t$.

$$\rho_{11}=\tfrac{1}{4}R_{1,1-1}{}^2(|F_{1,-1}|^2+|F_{11}|^2)/N_A, \tag{61b}$$

$$\rho_{22}=\tfrac{1}{2}(1-2\rho_{11}-\rho_{00}), \tag{61c}$$

$$\rho_{1,-1}=\tfrac{1}{2}R_{1,1-1}|F_{11}||F_{1,-1}|/N_A. \tag{61d}$$

### (c) $A_2$ Trajectory Exchange

The only result needed is the value of $\rho_{00}$,

$$\rho_{00}=0. \tag{62}$$

This prediction follows from the result that all helicity amplitudes with zero $f^0$ helicity are zero. However, experiment indicates[32,33] that $\rho_{00}$ is very close to its maximum value of 1, rather than being zero, so that $A_2$ trajectory exchange must contribute a very small fraction of the total amplitude.

Data exist on $f^0$ production at pion lab momenta of 4.0,[34] 6.0,[32] and 10.0[33] GeV/$c$. Examination of kinematics for these energies reveals that the high-energy approximations previously used are not at all valid, and the energy dependence of the $F_{\lambda\lambda'}$ functions must be considered. A comparison was made of the exact values for $F_{\lambda\lambda'}$ in this reaction with the $[(1\pm x)/2]^{(\lambda\pm\lambda')/2}s^{\alpha-\lambda}$ form. It was found that the difference is less than 7% for all $z$ values represented by the data. This is due mainly to the range of values of the trajectory and cannot be considered a general result. This brings in additional complications in determining the trajectory values from the data, since the $F_{\lambda\lambda'}$, which have different energy dependence, are multiplied by the unknown residue functions. The additional information on the ratios of these residue functions can be obtained from the spin density matrix elements $\rho_{00}$ and $\rho_{11}$ through Eqs. (58) or (61).

The trajectory values are determined by the iteration technique described in Sec. II. The final trajectory values were found to be roughly independent of the spin density matrix elements, as long as $0.8<\rho_{00}<1.0$, which is the range indicated by experiment. The validity of Regge-pole exchange is tested by the statistical uncertainty in the fit of the straight lines whose slopes determine the trajectory values. The results are: $A_1$ trajectory exchange converges to positive trajectory values approximately independent of $t$, but with very large errors, indicating that this exchange cannot explain the energy variation of the production cross section.

The $\pi$ trajectory exchange gives negative trajectory values which decrease with $t$ and have relatively small errors. These trajectory values are shown in Fig. 6, along with the parametrization,

$$\alpha_\pi(t)=-0.08\pm0.07+(0.69\pm0.29)t. \tag{63}$$

The conjecture that this is actually the trajectory associated with the $\pi$ is strengthened by the closeness of the zero intercept to the square of the pion mass. The trajectory could easily go through this point if given a small curvature, still consistent with the values determined.

The residue functions are determined by fitting the angular distribution at each energy and using the average values. The calculated cross sections are compared with the data in Fig. 7, and are seen to agree quite well.

The residue functions are approximately linear in $t$ for the range $-0.5\leq t\leq-0.05$ (GeV/$c$)$^2$:

$$10^{-6}R_{1,11}{}^2(t)=(0.01\pm0.05)-(0.86\pm0.15)t\ \mu\text{b}, \tag{64}$$

$$10^{-6}R_{0,11}{}^2(t)=(0.18\pm0.02)-(0.92\pm0.09)t\ \mu\text{b}. \tag{65}$$

Since the pion pole at $t=\mu^2=0.02$ (GeV/$c$)$^2$ is so close to the physical region, it is tempting to try to extrapolate the Regge formula to this point, and compare it with the field-theoretic expression for elementary pion exchange. In this limit, we have $F_{00}\to1$, $F_{10}$ and $F_{20}\to0$, $\alpha(t)\to0$, and $1+\cot^2(\pi\alpha/2)\to[2/\pi\alpha'(t-\mu^2)]^2$, where $\alpha'$ is the slope of the pion trajectory. This gives for the extrapolated cross section

$$\frac{d\sigma}{dt}\xrightarrow[t\to\mu^2]{}\frac{M^2R_{0,11}{}^2(t)}{16\pi[(s-M^2-\mu^2)^2-4M^2\mu^2](\alpha')^2(t-\mu^2)^2}. \tag{66}$$

[32] CERN-Ecole Polytechnique Collaboration, in *Proceedings of the 12th International Conference on High-Energy Physics*, edited by Ya. A. Smorodinsky (Atomizdat, Moscow, 1966), p. 442.

[33] M. Wahlig, E. Shibata, D. Goldon, D. Frisch, and I. Mannelli, Phys. Rev. **147**, 941 (1966); D. Gordon (private communication).

[34] German-British Collaboration, Nuovo Cimento **31**, 729 (1964).

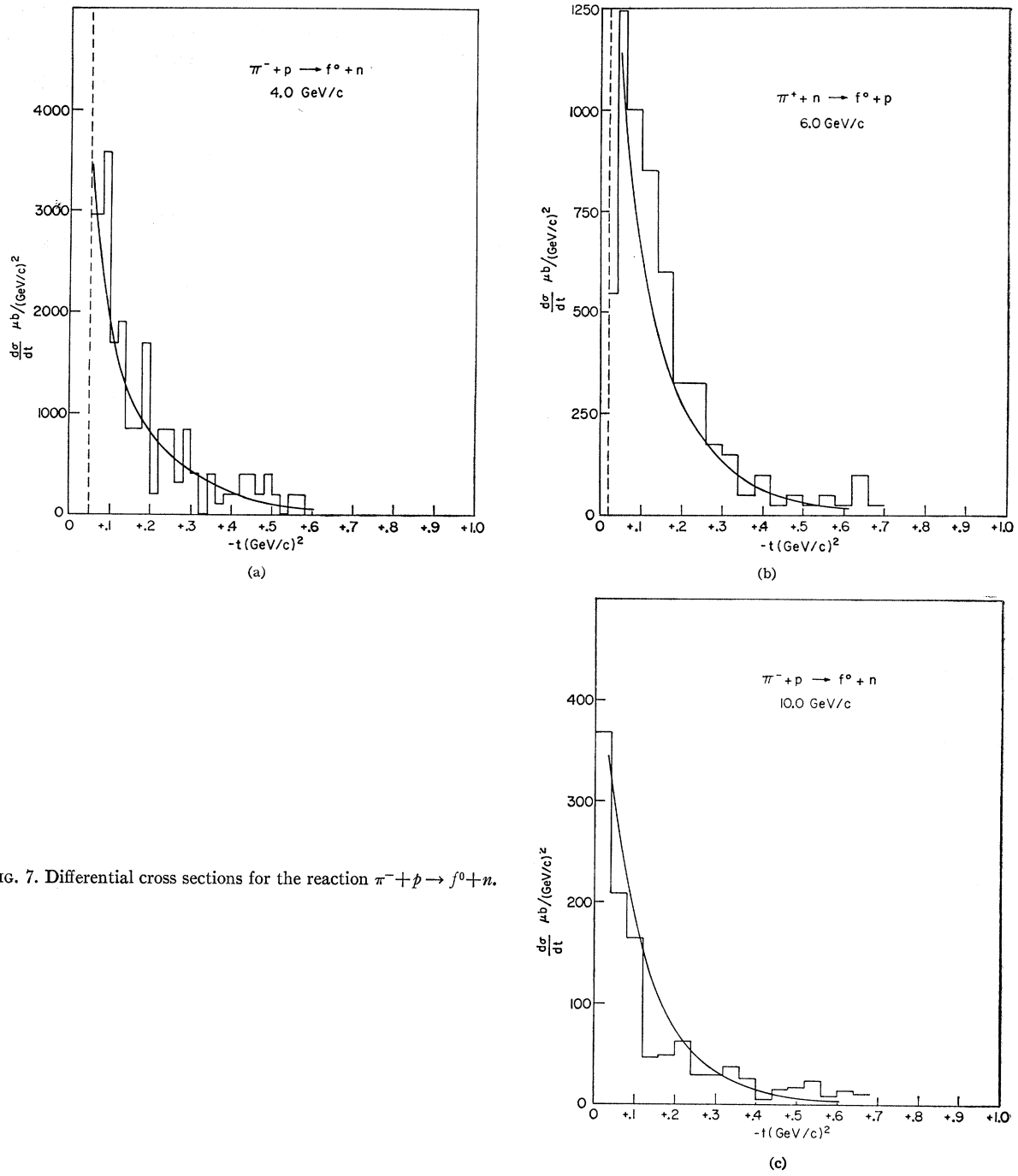


FIG. 7. Differential cross sections for the reaction $\pi^- + p \rightarrow f^0 + n$.

The field-theoretic cross section is

$$\frac{d\sigma}{dt} = \frac{G^2/4\pi}{(s-M^2-\mu^2)^2-4M^2\mu^2} \times \frac{(-t)}{(t-\mu^2)^2} \frac{40\pi}{3} \frac{(m_f)^2}{P} \Gamma_{f\rightarrow 2\pi}. \quad (67)$$

A useful quantity for the extrapolation is

$$\frac{R_{0,11}{}^2(t)}{-t} \underset{t\rightarrow\mu^2}{\longrightarrow} 40 \frac{G^2}{4\pi} \frac{(m_f)^2}{M^2} \frac{(\alpha')^2}{P} \frac{16\pi^2}{3} \Gamma_{f\rightarrow 2\pi}. \quad (68)$$

From (65), we see that this quantity would diverge at $t=0$ if the linear behavior of $R^2{}_{0,11}(t)$ were continued

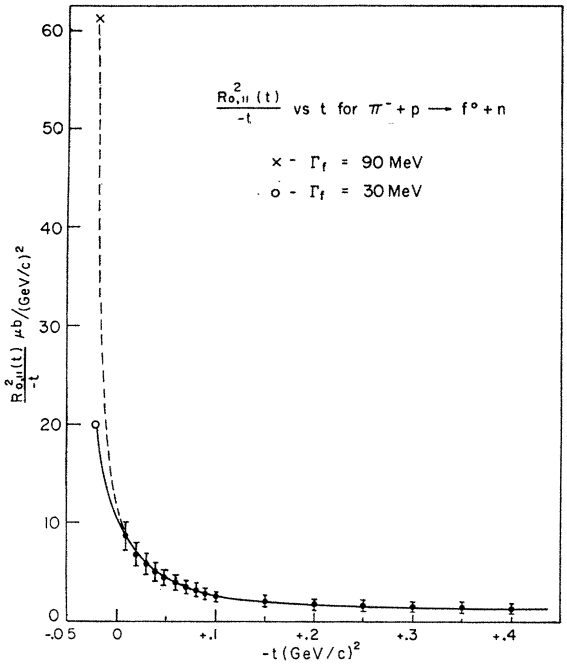


FIG. 8. Values of pion residue function from $f^0$ production data.

to $t>-0.05$ (GeV/$c$)$^2$. This factor of $t$ is expected to appear, owing to the kinematical singularities of helicity amplitudes for the $\pi N\bar{N}$ coupling,[35] along with factors of $[t-(\mu+m_f)^2]^{-1/2}$ and $[t-(\mu-m_f)^2]^{-1/2}$. The last two factors are slowly varying in the region of extrapolation and can be neglected. The $t$ factor should produce a minimum in the forward direction, but if it is there, the experimental resolution is evidently not fine enough to see it. Figure 8 shows a plot of $R_{0,11}{}^2(t)/(-t)$ in the physical region. The field-theoretic value at $t=\mu^2$ exceeds the residue function in the forward direction by as much as a factor of 10. The result is that even though the residue function is a slowly varying function of $t$ in the physical region, its extrapolation even a small distance outside this region is extremely uncertain. Of course, an exponential behavior can always be factored out of the residue function by changing the scale factor for the energy expansion, $(s/s_0)^\alpha$. This introduces a factor $\exp[2\alpha' \ln(s_0/s_0')(t-\mu^2)]$. However, to make the variation of the extrapolated function negligible between $t=\mu^2$ and $t=-0.1$ (GeV/$c$)$^2$, the scale factor must be changed by a factor of about 1800, which corresponds to $s_0=700$ (GeV)$^2$. This then spoils the slowly varying nature of the residue function in the physical region.

Now we turn to the reaction $\pi^\pm+p\rightarrow\rho^\pm+p$. Since the isospin of the $\rho$ is one, we can now have isospin zero exchanged particles, such as the $\omega$, as well as those allowed for $f^0$ production. Since the parity of the $\rho$ and $f^0$ both satisfy $P=(-1)^J$, we see from the derivation for $f^0$ production, that the expressions for $\pi$ and $A_1$ trajectory exchange can be taken over directly to $\rho$ production by neglecting the states with helicity $\pm2$. The contribution of the $A_2$ or $\omega$ trajectory can be calculated by using the parity conservation requirements on the $t$-channel helicity amplitudes for an intermediate particle with parity $(-1)^J$:

$$\langle\lambda_1\lambda_2|M^J|\beta\rangle=-\langle-\lambda_1-\lambda_2|M^J|\beta\rangle, \quad (69)$$
$$\langle\lambda_1\lambda_2|M^J|\beta\rangle=-\langle\lambda_1\lambda_2|M^J|-\beta\rangle,$$

which reduces the number of independent amplitudes from 12 to 2. The contribution to the cross section is

$$\frac{d\sigma}{dt}=\frac{M^2}{8[(s-M^2-\mu^2)^2-4M^2\mu^2]}\left(\frac{\Gamma(\alpha+\frac{3}{2})}{\Gamma(\alpha+1)}\right)^2$$
$$\times\left(1+\frac{\cot^2(\pi\alpha_R/2)}{\tan^2(\pi\alpha_\omega/2)}\right)\left(\frac{s-M^2-\frac{1}{2}(\mu^2+m_\rho{}^2-t)}{M(\mu m_\rho)^{1/2}}\right)^{2\alpha(t)}N_0, \quad (70)$$

where

$$N_0=R_{1,11}{}^2|F_{10}|^2+\tfrac{1}{2}R_{1,1-1}{}^2(|F_{11}|^2+|F_{1,-1}|^2). \quad (71)$$

The spin density matrix elements are

$$\rho_{00}=0, \quad (72a)$$
$$\rho_{11}=\tfrac{1}{2}, \quad (72b)$$
$$\rho_{1,-1}=(\tfrac{1}{2}R_{1,11}{}^2|F_{10}|^2-\tfrac{1}{2}R_{1,1-1}{}^2|F_{1-1}||F_{11}|)/N_0, \quad (72c)$$

and

$$\mathrm{Re}\rho_{10}=0. \quad (72d)$$

Experimental data exist for this reaction at pion lab momenta of 1.6,[36] 2.75[37], 4.0,[24] and 8.0[25,38] GeV/$c$. Measurements of $\rho_{00}$ indicate that it is in the range 0.5–0.8. This indicates that a large part of the amplitude must come from $\pi$ or $A_1$ exchange, since $\omega$ or $A_2$ exchange gives $\rho_{00}=0$.

A single trajectory fit was performed for the data, similar to that described for the $f^0$ case. The ratio of the residue functions was determined by the $\rho_{00}$ values at 4.0 GeV/$c$, and the same iteration technique was used to determine the trajectory values. The results are similar to those for the $f^0$ case. The $A_1$ trajectory values obtained had large statistical errors, indicating that they do not adequately represent the energy variation. The $\pi$ trajectory values had more reasonable errors, but they did not agree with those obtained from the $f^0$ reaction. They were consistently higher over the entire range of momentum transfer, even being positive for small momentum transfer. It seems that the amplitude must contain contributions from the $\omega$ or $A_2$ trajectories as well as the $\pi$.

The expression for the cross section including the $\pi$ trajectory and either the $\omega$ or the $A_2$ is just the sum of

[35] L.-L. Wang, Phys. Rev. **142**, 1187 (1966).

[36] Saclay-Orsay-Bari-Bologna Collaboration, Nuovo Cimento **29**, 515 (1963).

[37] Saclay-Orsay-Bari-Bologna Collaboration, Nuovo Cimento **37**, 361 (1965).

[38] Aachen-Berlin-CERN Collaboration, Phys. Letters **18**, 351 (1965).

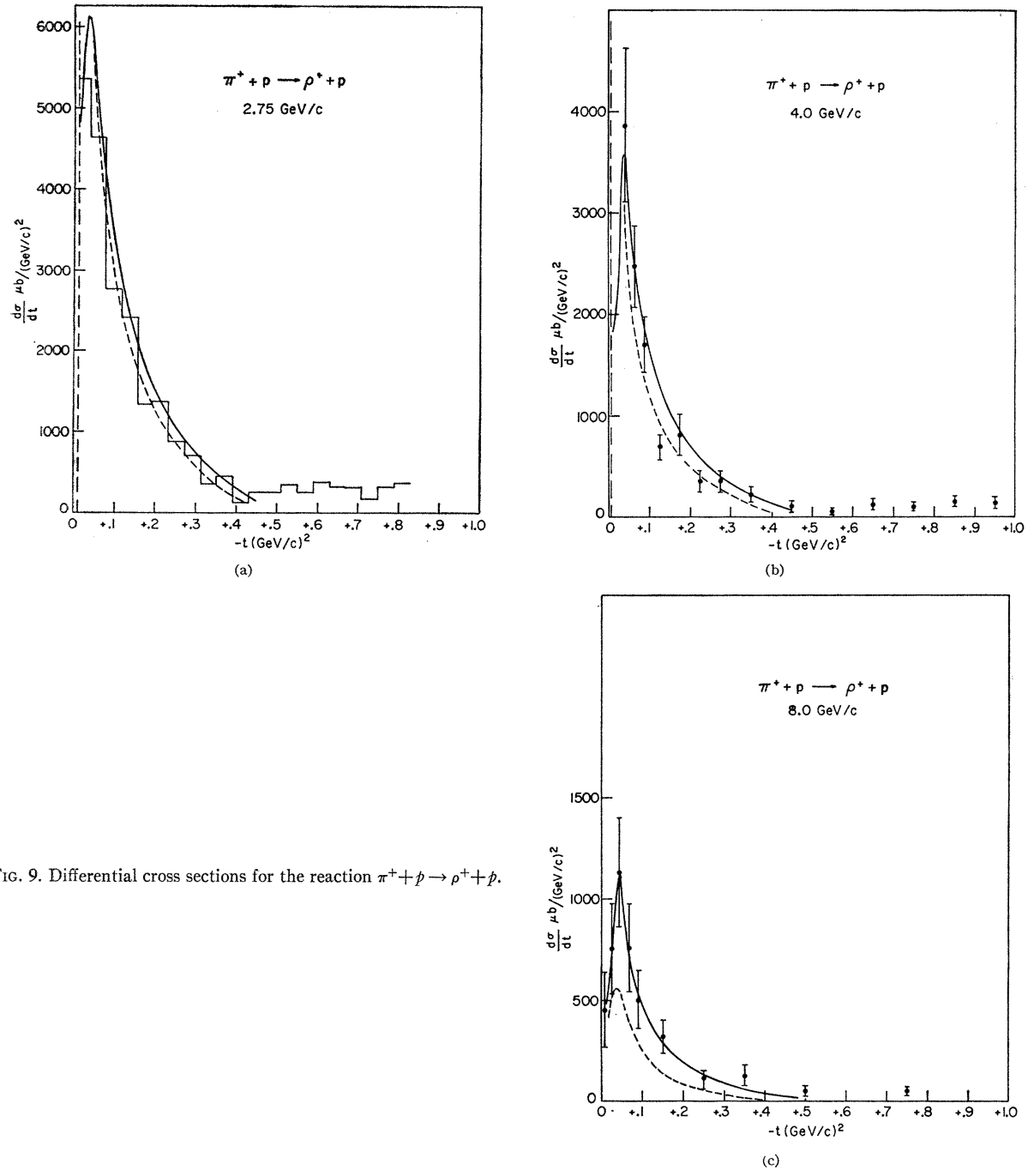


FIG. 9. Differential cross sections for the reaction $\pi^+ + p \rightarrow \rho^+ + p$.

the two separate contributions, since the interference term is zero. (See Appendix.) The $\rho_{00}$ values at 4 GeV/$c$ can be used to determine one of the $\pi$ residue functions $R_{0,11}{}^2(t)$, since this function gives the only contribution. [See 58(a).]

The $\pi$ trajectory values from $f^0$ production were used with this residue function to calculate the contribution of $\pi$ trajectory exchange. It was found to be about 80 to 90% of the experimental values for the low-energy data, dropping to about 50% for the 8-GeV/$c$ data. Thus the relative contribution from $\omega$ or $A_2$ exchange must increase with increasing energy, which is to be expected, since the largest trajectory values should dominate at high energy.

The second residue function for $\pi$ exchange, $R_{1,11}{}^2(t)$, must be small, since at low energies the contribution of the first function accounts for almost the total experimental value. An upper limit was calculated from data

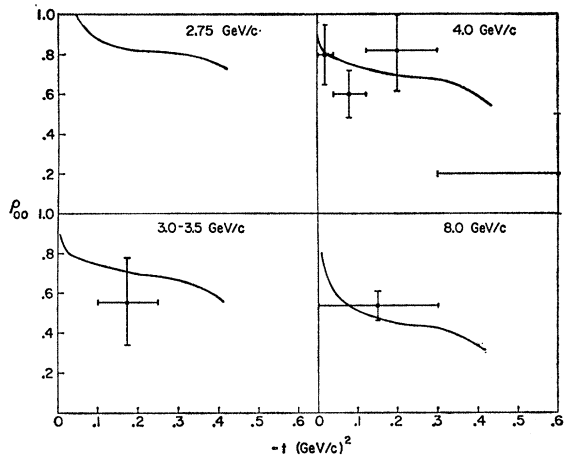


FIG. 10. Spin density matrix element $\rho_{00}$ for $\pi^+ + p \rightarrow \rho^+ + p$.

at 2.75 GeV/$c$, and the contribution to the cross section at higher energies was found to be very small ($<5\%$). The contribution due to $\pi$ trajectory exchange was subtracted from the experimental values, and the remainder was used in another single-Regge-pole calculation.

Since the difference is small, the percentage errors due to the experimental uncertainties are large, and no attempt was made to determine trajectory values from the data. Instead, trajectory values for the $\omega$ and $A_2$ were taken from the elastic and charge-exchange scattering analysis of Phillips and Rarita.[1] The two residue functions were determined by fitting the data at 4 GeV/$c$, and the results compared with the data at other energies through the Regge energy dependence. It was found that the $\omega$ exchange gives a contribution whose energy dependence fits the data better than that for $A_2$ exchange. The residue functions obtained were consistent with $R_{1,1-1}(t)=0$ for the $\omega$ exchange.

A calculation of the exact versus $s^{\alpha-\lambda}$ form of the $F_{\lambda\lambda'}$ functions again shows that they differ by less than

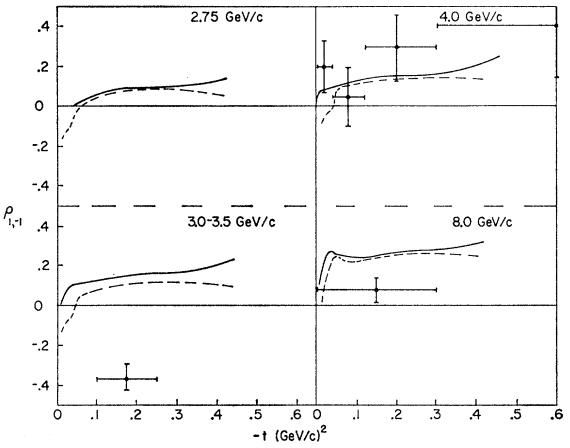


FIG. 11. Spin density matrix element $\rho_{1,-1}$ for $\pi^+ + p \rightarrow \rho^+ + p$.

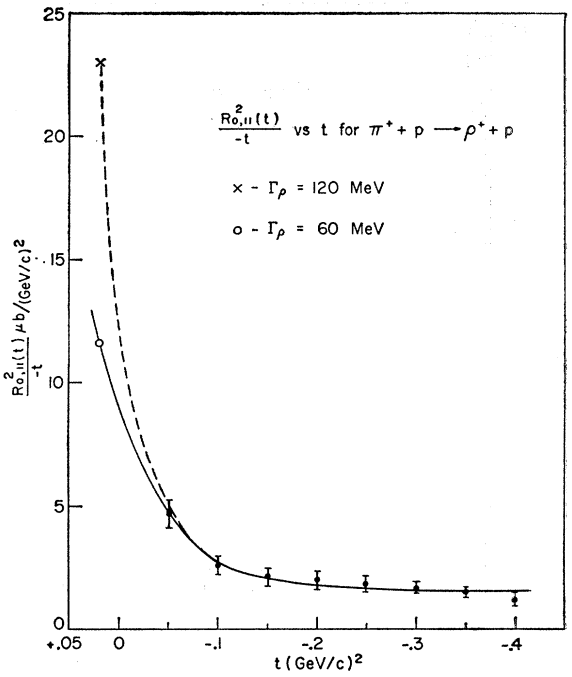


FIG. 12. Values of pion residue function from $\rho^+$ production data.

7%, but that the difference for those $\omega$ and $A_2$ amplitudes which were assumed to be consistent with zero is as great as a factor of two in some cases. In any event, the energy dependence of $d\sigma/dt$ needs a contribution with $\alpha(t)>0$, and the $\omega$ is taken as representative of this contribution.

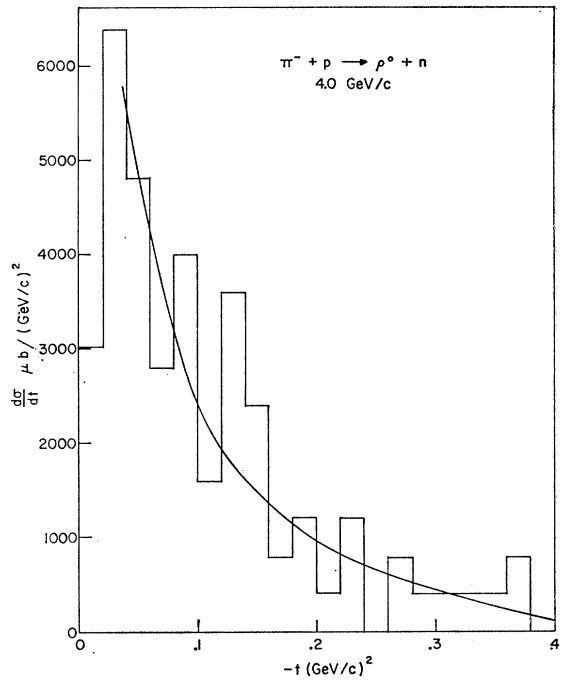


FIG. 13. Differential cross section for the reaction $\pi^+ + p \rightarrow \rho^0 + n$.

The $\omega$ trajectory values used were parametrized by $\alpha_\pi(t)=0.52+0.60t$. The comparison of the two-Regge-pole calculation ($\pi$ and $\omega$) with the data is shown in Fig. 9. The dashed lines indicate the $\pi$ contribution alone. The spin density matrix elements are shown in Figs. 10 and 11. The only values which were adjusted to fit the data were $\rho_{00}$ at 4 GeV/$c$; all other values are predicted by the Regge formula. The dashed lines for $\rho_{1,-1}$ are due to the inclusion of the small residue function $R^\pi{}_{1,11}(t)$. If it is not included, the solid lines are predicted. The element $\mathrm{Re}\rho_{10}$ is predicted to be zero from (58e) and (72d), and is in rough agreement with experiment, although a small nonzero value seems to be preferred. The measured values are $-0.074\pm0.070$ at 4.0 GeV/$c$,[24] and $-0.08\pm0.05$ at 8.0 GeV/$c$.[25]

The residue functions are again compared with the field-theoretic expression at the pion pole. The same type of derivation as for the $f^0$ case gives

$$\frac{R_{0,11}{}^2(t)}{-t}\xrightarrow[t\to u^2]{}\frac{G^2}{4\pi}\frac{(m_\rho)^2}{M^2}\frac{(\alpha')^2}{P_1}96\pi^2\Gamma_{\rho\to2\pi}. \tag{73}$$

The values are shown in Fig. 12, and again it is seen that the function must be rapidly varying in the forward direction, and the extrapolation is necessarily very inaccurate.

One additional prediction of the Regge-pole theory is that for the differential cross section for $\pi^-+p\to\rho^0+n$. The $\omega$ trajectory cannot be exchanged in this reaction, and isospin invariance requires that the $\pi$ trajectory contribution is twice that for the charged rho production. Data on $\rho^0$ production are available at 4.0 GeV/$c$,[34] and are compared with the predicted values in Fig. 13. The agreement supports the previous conclusion that $\pi$ exchange is predominant at this energy.

## ACKNOWLEDGMENTS

The author wishes to thank Professor Kerson Huang for suggesting this problem and for helpful discussion. He is also indebted to Dr. Y. Goldschmidt-Clermont for preliminary data on $Kp$ interactions, and to Dr. S. Nowak and Dr. D. R. O. Morrison for data on $\pi p$ interactions.

## APPENDIX

### Helicity Amplitudes

The helicity states of Jacob and Wick[9] are eigenstates of total angular momentum $J$ and the helicities of the individual particles $\lambda_1$ and $\lambda_2$. The parity operator acting on these states gives

$$P|J\lambda_1\lambda_2\rangle=P_1P_2(-1)^{J-S_1-S_2}|J,-\lambda_1-\lambda_2\rangle, \tag{A1}$$

where $P_1$, $P_2$, $S_1$, and $S_2$ are the parities and spins of the two particles. If parity is conserved, this leads to a relation between helicity amplitudes:

$$\langle-\lambda_3-\lambda_4|M^J|-\lambda_1-\lambda_2\rangle=\frac{P_1P_2}{P_3P_4}(-1)^{S_3+S_4-S_1-S_2}\langle\lambda_3\lambda_4|M^J|\lambda_1\lambda_2\rangle. \tag{A2}$$

If, in addition, the reaction proceeds through a one, particle state with definite parity $\mathcal{P}$, we have

$$\langle\lambda_3\lambda_4|M^J|-\lambda_1-\lambda_2\rangle=\sigma\langle\lambda_3\lambda_4|M^J|\lambda_1\lambda_2\rangle, \tag{A3}$$

where

$$\sigma=-P_1P_2(-1)^{S_1+S_2}\quad\text{if}\quad\mathcal{P}=(-1)^J,$$

and

$$\sigma=+P_1P_2(-1)^{S_1+S_2}\quad\text{if}\quad\mathcal{P}=-(-1)^J.$$

This leads to the result that the interference term for exchanged particles (or trajectories) of opposite $J$ parity does not contribute to the spin-averaged differential cross section, in the high-energy approximation.

Further restrictions on helicity amplitudes come from $G$ parity conservation, if one of the external states is a particle-antiparticle system. Since $G=Ce^{i\pi T_2}$, we are interested in charge-conjugation properties. For a particle-antiparticle system, charge conjugation is equivalent to interchange of particles, and[9]

$$P_{12}|J\lambda_1\lambda_2\rangle=(-1)^{J-2S}|J\lambda_2\lambda_1\rangle. \tag{A4}$$

The rotation in isospin space just gives a factor $(-1)^T$ for a state with total isospin $T$, so the result is

$$G|J\lambda_1\lambda_2\rangle=(-1)^{T+J-2S}C_1C_2|J\lambda_2\lambda_1\rangle. \tag{A5}$$

For a $K\bar{K}$ system, this implies that $G=(-1)^{T+J}$.

For an $N\bar{N}$ system, this relation together with parity conservation leads to restrictions on the helicity amplitudes $M_{2\lambda_1,2\lambda_2}$, which are presented in Table I.

TABLE I. Restrictions on helicity amplitudes from $G$ parity conservation.

| $G(-1)^T$ | $J$ | $P$ | Restrictions |
|---|---|---|---|
| $+1$ | even | $+1$ | $M_{11}=M_{-1-1}$ |
| $-1$ | odd | $-1$ | $M_{1-1}=M_{-1,1}$ |
| $+1$ | even | $-1$ | $M_{11}=-M_{-1-1}$ |
| $-1$ | odd | $+1$ | $M_{1-1}=M_{-1,1}=0$ |
| $+1$ | odd | $+1$ | $M_{11}=M_{-1-1}=0$ |
| $-1$ | even | $-1$ | $M_{1-1}=-M_{-1,1}$ |
| $+1$ | odd | $-1$ | All $M_{2\lambda_1,2\lambda_2}=0$ |
| $-1$ | even | $+1$ | |

### Rotation Coefficients

The rotation coefficients of the first kind, $d^J{}_{\lambda\lambda'}(z)$, can be continued to complex $J$ by their relation with the hypergeometric function[10]:

$$d^J{}_{\lambda\lambda'}(z)=\left[\frac{\Gamma(J+\lambda+1)\Gamma(J-\lambda'+1)}{\Gamma(J-\lambda+1)\Gamma(J+\lambda'+1)}\right]^{1/2}\left(\frac{1+z}{2}\right)^{(\lambda+\lambda')/2}\left(\frac{1-z}{2}\right)^{(\lambda-\lambda')/2}\frac{F(\lambda-J,\,\lambda+J+1,\,\lambda-\lambda'+1,\,(1-z)/2)}{\Gamma(\lambda-\lambda'+1)}. \quad \text{(A6)}$$

A similar relation holds for the rotation coefficients of the second kind:

$$e^J{}_{\lambda\lambda'}(z)=\frac{1}{2}\frac{[\Gamma(J+\lambda+1)\Gamma(J+\lambda'+1)\Gamma(J-\lambda'+1)\Gamma(J-\lambda+1)]^{1/2}}{\Gamma(2J+2)}$$

$$\times\left(\frac{1+z}{2}\right)^{-(\lambda+\lambda')/2}\left(\frac{1-z}{2}\right)^{-(\lambda-\lambda')/2}\left(\frac{z-1}{2}\right)^{-J-\lambda'-1}F(J+\lambda+1,\,J+\lambda'+1,\,2J+2,\,2/(1-z)). \quad \text{(A7)}$$

The integral relation between them is

$$\int_{-1}^{1}\frac{dt}{z-t}\left(\frac{1+t}{2}\right)^{(\lambda+\lambda')/2}\left(\frac{1-t}{2}\right)^{(\lambda-\lambda')/2}d^J{}_{\lambda\lambda'}(t)=2\left(\frac{1+z}{2}\right)^{(\lambda+\lambda')/2}\left(\frac{1-z}{2}\right)^{(\lambda-\lambda')/2}e^J{}_{\lambda\lambda'}(z), \quad \text{(A8)}$$

for $J\geq\lambda\geq|\lambda'|$. The final form of the rotation coefficients used in the Regge-pole calculations is obtained by using the relations

$$F(a,b,c,z)=(1-z)^{-a}F\left(a,\,c-b,\,c,\,\frac{z}{z-1}\right), \quad \text{(A9)}$$

$$\frac{d^n}{dz^n}[z^{a+n+1}F(a,b,c,z)]=\frac{\Gamma(a+n)}{\Gamma(a)}z^{a-1}F(a+n,\,b,\,c,\,z), \quad \text{(A10)}$$

and

$$F(a,b,2b,z)=(1-\tfrac{1}{2}z)^{-a}F\left(\frac{a}{2},\,\frac{1+a}{2},\,b+\tfrac{1}{2},\,\frac{z^2}{(2-z)^2}\right). \quad \text{(A11)}$$

The final form of the rotation coefficients is a product of $(-2z)^\alpha$ times the function $F_{\lambda\lambda'}(\alpha,z)$. For $\alpha<0$, the function is

$$F_{\lambda\lambda'}(\alpha,z)=f_{\lambda\lambda'}\left[g^{(1)}{}_{\lambda\lambda'}F\left(-\frac{\alpha}{2},\,\frac{1-\alpha}{2},\,\tfrac{1}{2}-\alpha,\,\frac{1}{z^2}\right)+h^{(1)}{}_{\lambda\lambda'}F'\left(-\frac{\alpha}{2},\,\frac{1-\alpha}{2},\,\tfrac{1}{2}-\alpha,\,\frac{1}{z^2}\right)\right], \quad \text{(A12)}$$

TABLE II. Expansion functions for rotation coefficients.

| $\lambda$ | $\lambda'$ | $f_{\lambda\lambda'}$ | $g_{\lambda\lambda'}{}^{(1)}$ | $h_{\lambda\lambda'}{}^{(1)}$ | $g_{\lambda\lambda'}{}^{(2)}$ | $h_{\lambda\lambda'}{}^{(2)}$ |
|---|---|---|---|---|---|---|
| 0 | 0 | $1$ | $1$ | $0$ | $1$ | $0$ |
| 1 | 0 | $i\left[\frac{\alpha}{\alpha+1}\left(1-\frac{1}{z^2}\right)\right]^{\frac{1}{2}}$ | $1$ | $\frac{-2}{\alpha z^2}$ | $-1-\frac{1}{\alpha}$ | $\frac{-2}{\alpha z^2}$ |
| 1 | 1 | $\frac{-1}{\alpha+1}$ | $\alpha+\frac{1}{z}$ | $\frac{-2(1-z)}{\alpha z^3}$ | $\alpha+\frac{1}{z}-\frac{(2\alpha+1)(1-z)}{\alpha z}$ | $\frac{-2(1-z)}{\alpha z^3}$ |
| 1 | $-1$ | $\frac{1}{(\alpha+1)}$ | $\alpha-\frac{1}{z}$ | $\frac{2(1+z)}{\alpha z^3}$ | $\alpha-\frac{1}{z}+\frac{(2\alpha+1)(1+z)}{\alpha z}$ | $\frac{2(1+z)}{\alpha z^3}$ |
| 2 | 0 | $-\left[\frac{\alpha(\alpha-1)}{(\alpha+1)(\alpha+2)}\right]^{\frac{1}{2}}$ | $1$ | $\frac{4}{\alpha(\alpha-1)z^2}$ | $1+\frac{2(2\alpha+1)}{\alpha(\alpha-1)}$ | $\frac{4}{\alpha(\alpha-1)z^2}$ |

where $F'$ denotes the derivative of the hypergeometric function with respect to its argument. For $\alpha>0$, $F_{\lambda\lambda'}$ contains some additional terms which are written as

$$\left[\frac{\Gamma(\alpha+1)}{\Gamma(\alpha+\frac{1}{2})}\right]^2 \frac{\tan\pi\alpha}{(\alpha+\frac{1}{2})(-2z)^{2\alpha+1}}\left[g^{(2)}_{\lambda\lambda'}F\left(1+\frac{\alpha}{2},\ \tfrac{1}{2}+\alpha,\ \alpha+\tfrac{3}{2},\ \frac{1}{z^2}\right)+h^{(2)}_{\lambda\lambda'}F'\left(1+\frac{\alpha}{2},\ \tfrac{1}{2}+\alpha,\ \alpha+\tfrac{3}{2},\ \frac{1}{z^2}\right)\right]. \quad \text{(A13)}$$

The functions $f_{\lambda\lambda'}$, $g_{\lambda\lambda'}{}^{(1,2)}$, and $h_{\lambda\lambda'}{}^{(1,2)}$ are tabulated for some small values of $\lambda$ and $\lambda'$ in Table II.

PHYSICAL REVIEW VOLUME 155, NUMBER 5 25 MARCH 1967

# Daughter Trajectories and Unequal-Mass Scattering*

DANIEL Z. FREEDMAN, C. EDWARD JONES,† AND JIUNN-MING WANG
*Lawrence Radiation Laboratory, University of California, Berkeley, California*
(Received 26 September 1966)

It has recently been demonstrated by Goldberger and Jones (I) and by Freedman and Wang (II) that Regge asymptotic behavior obtains at high energy even in regions in which the crossed-channel $\cos\theta$ variable is constrained by unequal-mass kinematics to remain finite. Approaches I and II differ, however, in other important respects. In this note it is shown that method I can be adapted and used to prove the existence and properties of the Regge daughter trajectories found in II. In this argument, an extra assumption necessary in II is avoided, and the restriction $\alpha(0)<\frac{1}{2}$ found in I is eliminated.

RECENTLY two different arguments have been given to show that the Regge asymptotic behavior $u^{\alpha(s)}$ is maintained in the backward scattering of unequal-mass particles even though the cosine of the $u$-channel scattering angle remains small.[1,2] In both methods the persistence of the behavior $u^{\alpha(s)}$ is a consequence of the analyticity of the full amplitude at $s=0$, a property not shared by the individual Regge-pole terms.

In I, dispersion relations are used to correct the analyticity of the original Regge pole terms, whereas in II a representation of the scattering amplitude as the Sommerfeld-Watson transform of power series in the Mandelstam variables $u$ and $t$, called the Khuri representation, is employed. For the asymptotic contribution at $s=0$ of the leading Regge pole $\alpha_0(s)$, both methods find the dominant term $\gamma(0)u^{\alpha_0(0)}$ and the next dominant term $s^{-1}u^{\alpha_0(0)-1}$, which has an $s^{-1}$ singularity not shared by the full amplitude and which must, therefore, be cancelled.

The main difference between I and II lies in the mechanism by which this singularity is cancelled. In I it is argued that the singularity is cancelled by the background term of the Regge representation, and the restriction $\alpha_0(0)<\frac{1}{2}$ is therefore found. In II it is argued that the singularity is cancelled by contributions of other Regge poles, and it is found that to effect this cancellation there must occur daughter trajectories $\alpha_k(s)$, correlated with the leading or parent trajectory by the conditions $\alpha_k(0)=\alpha_0(0)-k$. No restriction on the position of the leading trajectory stronger than that of Froissart [namely, $\alpha_0(0)\leqslant 1$] is found. Mathematically there does not seem to be any *a priori* reason to prefer either mechanism, but it is found in II that the daughter trajectory mechanism is satisfied in all Bethe-Salpeter models which Reggeize, and empirically it is known that the Pomeranchuk trajectory violates the constraint $\alpha(0)<\frac{1}{2}$.

The analyticity of the Khuri power-series coefficients at $s=0$ is important to the argument of II. It was made plausible there but not rigorously proved, and was left as an extra assumption. The purpose of this article is to show that the existence and properties of the first daughter trajectory can be proved without such an extra assumption by using the techniques of I and demanding consistency between the Regge representation and Mandelstam analyticity in the case where there are Regge poles to the right of $\mathrm{Re}l=\frac{1}{2}$ for $s=0$. In this way we eliminate the restriction $\alpha(0)<\frac{1}{2}$ and asymptotic fixed powers larger than background (see I).

It is not clear how to take the Regge background integral to the left of $\mathrm{Re}l=-\frac{1}{2}$ with this technique because of the threshold accumulation of poles there, and therefore the discussion of lower-lying daughter trajectories from this point of view may be difficult.

In the treatment here we rely heavily on references to I and II. For simplicity we follow I in assuming that

* Work done under the auspices of the U. S. Atomic Energy Commission.
† Present address: Physics Department, M.I.T., Cambridge, Massachusetts.
[1] M. L. Goldberger and C. E. Jones, Phys. Rev. **150**, 1269 (1966); referred to as I. Also Phys. Rev. Letters **17**, 105 (1966).
[2] D. Z. Freedman and J. M. Wang, Phys. Rev. **153**, 1596 (1967); referred to as II. See also Phys. Rev. Letters **17**, 569 (1966).